

# Critical Review of Pd-Based Catalytic Treatment of Priority Contaminants in Water

Brian P. Chaplin,<sup>†</sup> Martin Reinhard,<sup>‡</sup> William F. Schneider,<sup>§</sup> Christoph Schüth,<sup>||</sup> John R. Shapley,<sup>⊥</sup> Timothy J. Strathmann,<sup>¶</sup> and Charles J. Werth<sup>\*,||</sup>

<sup>†</sup>Department of Civil and Environmental Engineering and Villanova Center for the Advancement of Sustainable Engineering, Villanova University, Villanova, Pennsylvania 19085, United States

<sup>‡</sup>Department of Civil and Environmental Engineering, Yang and Yamasaki Environment and Energy Building, 473 Via Ortega, Stanford University, Stanford, California 94305, United States

<sup>§</sup>Department of Chemical and Biomolecular Engineering and Department of Chemistry and Biochemistry, University of Notre Dame, Notre Dame, Indiana 46556, United States

<sup>||</sup>Institute of Applied Geosciences, Technische Universität Darmstadt, Schnittspahnstrasse 9, D-64287 Darmstadt, Germany

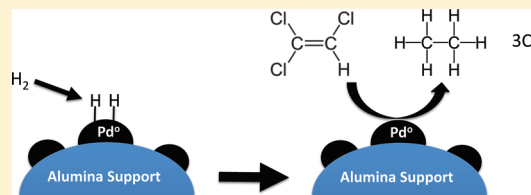
<sup>⊥</sup>Department of Chemistry, University of Illinois at Urbana–Champaign, Urbana, Illinois 61801, United States

<sup>¶</sup>Department of Civil and Environmental Engineering, University of Illinois at Urbana–Champaign, Urbana, Illinois 61801, United States

## S Supporting Information

**ABSTRACT:** Catalytic reduction of water contaminants using palladium (Pd)-based catalysts and hydrogen gas as a reductant has been extensively studied at the bench-scale, but due to technical challenges it has only been limitedly applied at the field-scale. To motivate research that can overcome these technical challenges, this review critically analyzes the published research in the area of Pd-based catalytic reduction of priority drinking water contaminants (i.e., halogenated organics, oxyanions, and nitrosamines), and identifies key research areas that should be addressed.

Specifically, the review summarizes the state of knowledge related to (1) proposed reaction pathways for important classes of contaminants, (2) rates of contaminant reduction with different catalyst formulations, (3) long-term sustainability of catalyst activity with respect to natural water foulants and regeneration strategies, and (4) technology applications. Critical barriers hindering implementation of the technology are related to catalyst activity (for some contaminants), stability, fouling, and regeneration. New developments overcoming these limitations will be needed for more extensive field-scale application of this technology.



## 1. INTRODUCTION

Palladium (Pd)-based catalysis has emerged as a promising water treatment strategy, as supported-Pd and Pd-based bimetallic catalysts can activate dihydrogen ( $H_2$ ) and catalyze reductive transformation of a number of priority drinking water contaminants (Figure 1).

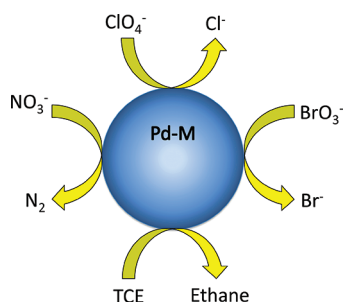
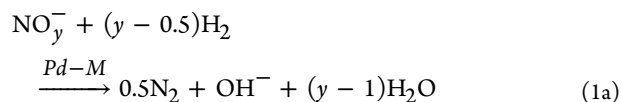


**Figure 1.** Schematic showing the transformation of  $NO_3^-$ ,  $ClO_4^-$ ,  $BrO_3^-$ , and trichloroethylene (TCE) on a Pd-M catalyst particle (M = Cu, In, Re). Only select important products are shown.

Of particular regulatory interest are oxyanions (e.g., nitrate ( $NO_3^-$ ), nitrite ( $NO_2^-$ ), bromate ( $BrO_3^-$ ), chlorate ( $ClO_3^-$ ), and perchlorate ( $ClO_4^-$ )),<sup>1–6</sup> *N*-nitrosamines (e.g., *N*-nitrosodimethylamine (NDMA)),<sup>7,8</sup> and a number of halogenated alkanes (e.g., carbon tetrachloride (CT), 1,2-dichloroethane),<sup>9–12</sup> alkenes (e.g., trichloroethylene (TCE), perchloroethene (PCE)),<sup>9–12</sup> and aromatics (e.g., chlorinated benzenes, polychlorinated biphenyls (PCBs)).<sup>12–14</sup> For example, the nitrogen oxyanions are catalytically reduced to dinitrogen ( $N_2$ ) and ammonia ( $NH_3$ ):

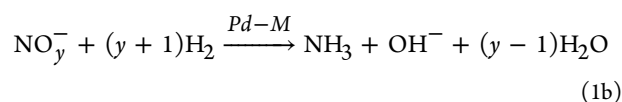


**Received:** November 15, 2011

**Revised:** February 24, 2012

**Accepted:** February 27, 2012

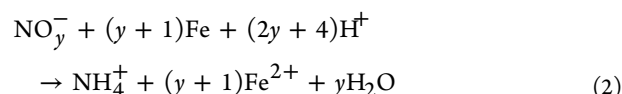
**Published:** February 27, 2012



Key practical challenges are to maximize the activity and selectivity toward desired reduction products ( $\text{N}_2$  in this case), improve the resistance toward catalyst fouling, and design reactors for full-scale applications.

Metals besides Pd have also been explored for catalytic contaminant reduction. These include supported Pt, Ir, Rh, Cu, Zn, Ru (alone or with a promoter metal), and various forms of Ni.<sup>15–23</sup> In general, Pd-based catalysts are more active, stable, and selective for desired end products, and/or less toxic. For example, Pt- and Pd-based catalysts have shown similar initial  $\text{NO}_3^-$  reduction activities but Pt was more susceptible to deactivation over time and exhibited a higher selectivity to  $\text{NH}_4^+$ .<sup>20</sup> Pt-based catalysts also show lower activity for dehalogenation than do Pd-based catalysts.<sup>21</sup> Rh-based catalysts similarly have higher selectivity toward  $\text{NH}_4^+$  but have been reported to have both higher and lower activity than Pd for  $\text{NO}_3^-$  reduction.<sup>22,24–26</sup> Rh activities toward dehalogenation are lower than Pd.<sup>21</sup> Ni-based catalysts have shown both higher and lower activity than Pd-based catalysts for  $\text{NO}_3^-$  reduction and dehalogenation.<sup>18,22,23</sup> Ni-based catalysts are reported to have an approximate 3–6 fold increase in activity relative to Pd monometallic catalysts for NDMA reduction, and a similar activity to Pd–Cu and Pd–In catalysts.<sup>7,8,27,28</sup> However, Ni leaching is a serious concern,<sup>29,30</sup> selectivity for  $\text{NH}_4^+$  during  $\text{NO}_3^-$  reduction is typically high,<sup>18</sup> Ni is unstable when exposed to oxidants<sup>31</sup> (preventing catalyst regeneration), and Raney-Ni (a highly active form) is pyrophoric when dry and considered dangerous to handle in air.<sup>32</sup> Various monometallic and bimetallic catalysts other than Pd have been tested for catalytic reduction of  $\text{ClO}_4^-$  (e.g., Pt/C, Ni–Pt/C, Co–Pt/C, W–Pt/C, Ru/C, W/C, and Raney-Ni), but rates are generally slow, e.g., taking days to observe appreciable  $\text{ClO}_4^-$  reduction.<sup>33,34</sup> Although recent electrocatalytic reduction methods appear promising,<sup>35,36</sup> electrochemical reduction is outside the scope of this review.

There are a variety of other, noncatalytic, approaches to remediating these priority drinking water contaminants. Direct reduction through stoichiometric reaction with an active metal, most commonly zerovalent iron (ZVI), has been explored, which leads primarily to  $\text{NH}_4^+$  production:



ZVI is advantageous because it is inexpensive, readily available as a scrap metal, oxidized to naturally occurring soil mineral products that are relatively nontoxic, and inherently a reducing agent. However, reduction rates for common contaminants using ZVI are typically orders of magnitude less than with catalytic metals,<sup>7,37,38</sup> and selectivity for  $\text{NH}_4^+$  instead of  $\text{N}_2$  during  $\text{NO}_3^-$  and NDMA reduction is high.<sup>7,38</sup> For example,  $\text{NO}_3^-$  reduction by ZVI has been reported to be 100% selective for  $\text{NH}_4^+$ .<sup>38</sup> Although  $\text{NH}_4^+$  selectivity of <10% during Pd bimetallic reduction of  $\text{NO}_3^-$  has been reported,<sup>39–41</sup> limiting  $\text{NH}_4^+$  production during catalytic  $\text{NO}_3^-$  reduction is still a primary focus of applied research. The use of nm-size ZVI particles enhances rates relative to  $\mu\text{m}$ -size particles,<sup>42</sup> but mass-normalized rates are still approximately an order of

magnitude lower than catalytic reduction.<sup>43</sup> Additionally, ZVI forms deactivating surface oxides that may reduce long-term effectiveness in remediation applications.<sup>44,45</sup>

Conventional technologies used to treat priority contaminants include adsorption onto activated carbon (e.g., for halogenated organics) or ion exchange resins (e.g., for oxyanions), air stripping (e.g., for volatile organics), and oxidative and photolytic transformation (e.g., UV photolysis for NDMA).<sup>46</sup> Adsorption and air stripping processes transfer the contaminants from water to another phase, and disposal in a landfill or further contaminant treatment is required. Many chemical oxidants have poor selectivity for target contaminants and reactions with dissolved organic matter (DOM) consume the oxidant and can lead to a variety of toxic byproducts.<sup>47–51</sup> Contaminant treatment by UV photolysis typically requires UV light fluences that are an order of magnitude higher than those for disinfection.<sup>49</sup> Biological reduction can effectively reduce several contaminants (e.g.,  $\text{NO}_3^-$ ,  $\text{NO}_2^-$ ,  $\text{ClO}_4^-$ , and chlorinated organics).<sup>52–54</sup> Membrane bioreactors provide a barrier between microorganisms and treated water, alleviating concerns over pathogen release into water that have slowed implementation of biological reduction in drinking water treatment. Disadvantages of biological systems are potentially long startup times (e.g., weeks) and challenges associated with maintaining active biomass during intermittent operations.<sup>53</sup> The drawbacks of conventional technologies and biological reduction stimulate research and development efforts in catalytic reduction.

This review focuses on published research in the area of catalytic reduction of priority drinking water contaminants using Pd-based catalysts. We summarize the state of knowledge related to (1) proposed reaction pathways for important classes of contaminants, (2) rates of contaminant reduction with different catalyst formulations, (3) long-term sustainability with respect to natural water foulants, microbial fouling processes, and fouling prevention and regeneration strategies, and (4) technology applications. Catalyst formulations of interest include metallic Pd,<sup>10</sup> Pd on a variety of supports, e.g., alumina, silica, activated carbon, zeolites, or nanosized supports such as magnetite<sup>55,56</sup> and Au,<sup>57–60</sup> and supported bimetallic catalysts that include Pd plus promoter metals such as Cu,<sup>1,61</sup> Sn,<sup>62</sup> In,<sup>62</sup> or Re.<sup>4–6</sup> Although outside the scope of this review, Pd has also been added to ZVI in order to eliminate the need for an external  $\text{H}_2$  source (i.e., ZVI corrosion forms  $\text{H}_2$ ), and potentially enhance reaction rates.<sup>63–65</sup> We identify advantages and disadvantages of Pd-based catalytic reduction and prioritize future research directions necessary for widespread implementation of these technologies in water treatment and remediation. There are several excellent reviews available on Pd-based catalytic reduction of water contaminants.<sup>66–72</sup> This review spans contaminant classes and critically assesses the state of knowledge regarding catalytic transformation pathways and catalyst fouling and regeneration.

## 2. STATE OF KNOWLEDGE

**2.1. Proposed Reaction Pathways.** Proposed reaction pathways for catalytic reduction of several priority contaminants in water are illustrated in Table 1 and Table S-1 (Supporting Information). The reactions fall into three categories: (1) hydrodehalogenation for halogenated organics, (2) hydrodeoxygenation for oxyanions, and (3) N–N hydrogenolysis for N-nitrosamines. Many halogenated organics and some oxyanions (e.g.,  $\text{NO}_2^-$ ,  $\text{BrO}_3^-$ ,  $\text{ClO}_3^-$ ) can be reduced on Pd alone,<sup>1,10,73</sup> whereas  $\text{NO}_3^-$  and  $\text{ClO}_4^-$  reduction require a

Table 1. Proposed Reaction Pathways for Example Contaminants in Water<sup>a</sup>

Mechanism	Contaminants	Illustration of Proposed Reaction Pathways
Hydrodehalogenation	Chlorinated, iodated, and brominated organic compounds (e.g., carbon tetrachloride, trichloroethene, diatrizoate)	<p><u>Chlorinated ethene</u></p> <p><u>Carbon tetrachloride</u></p>
Hydrodeoxygenation	Oxanions (e.g., nitrate, nitrite, bromate, perchlorate, and chlorate)	<p><u>Perchlorate</u></p> <p><u>Nitrate</u></p>
N-N Hydrogenolysis	NDMA Azo dyes (e.g., methyl orange)	<p><u>NDMA</u></p>

<sup>a</sup>For the carbon tetrachloride reaction pathway, the boxes with dashed lines represent proposed, not observed, intermediates. Reaction pathways are not balanced reactions, but instead show important products that are formed. References for proposed reaction pathways: chlorinated ethenes,<sup>9</sup> chlorinated ethanes,<sup>10</sup>  $\text{ClO}_4^-$ ,<sup>4</sup>  $\text{NO}_3^-$ ,<sup>1,61,154</sup> and NDMA.<sup>8,165</sup>

secondary “promoter” metal.<sup>1,4</sup> Common promoter metals for  $\text{NO}_3^-$  are Cu, Sn, and In,<sup>1,15,62,74–76</sup> whereas Re promotes  $\text{ClO}_4^-$  reduction.<sup>3–6</sup> There is also evidence that for some contaminants amenable to reduction on Pd alone, reduction is faster on Pd bimetallic catalysts. NDMA is an excellent example; addition of 0.3 wt % Cu to a 1.0 wt % Pd/ $\gamma\text{-Al}_2\text{O}_3$  catalyst and 1.0 wt % In to a 5.0 wt % Pd/ $\gamma\text{-Al}_2\text{O}_3$  catalyst increased reduction rate constants 6- and 4-fold, respectively.<sup>7,8</sup>

Pd and a hydrogen/electron donor (typically  $\text{H}_2$ ) are essential to all three reaction categories. Metallic Pd can dissociatively adsorb  $\text{H}_2$  into adsorbed surface hydrogen ( $\text{Pd-H}_{\text{ads}}$ ), activating hydrogen for reductive chemistry with coadsorbed substrates.<sup>77</sup> Because Pd also has a high affinity for absorbing hydrogen,<sup>78,79</sup> the thermodynamic stability of  $\text{Pd-H}_{\text{ads}}$  is different for Pd nanoparticles vs bulk Pd, and calculations suggest that it depends on particle size.<sup>80,81</sup> For acetylene hydrogenation, “subsurface hydrogen” has been suggested to affect the relative energies of surface adsorbates and hence the selectivity of competing reaction pathways.<sup>82</sup> Possible roles for subsurface hydrogen in affecting the activity/selectivity of other reactions catalyzed by Pd nanoparticles are largely undefined.

A promoter metal is required for reduction of some contaminants. Promoter metals do not generally dissociate  $\text{H}_2$ , as evidenced by their inability to reduce contaminants in the absence of Pd.<sup>1,3</sup> Instead, they facilitate reduction by using “spillover”  $\text{Pd-H}_{\text{ads}}$ .<sup>83</sup> Ex situ X-ray photoelectron spectroscopy (XPS) data of a Pd–Re/C catalyst used for  $\text{ClO}_4^-$  reduction indicate that Pd was in the metallic state,<sup>84</sup> suggesting that for this contaminant Pd promotes  $\text{H}_2$  dissociation and the transfer of  $\text{Pd-H}_{\text{ad}}$  to the substrate via the Re center. Direct evidence from low-temperature scanning tunneling microscopy (STM) and density functional theory (DFT) calculations indicate that  $\text{Pd-H}_{\text{ads}}$  spills over from Pd onto the adjacent promoter metal.<sup>83</sup> The exact juxtaposition of Pd and the promoter metal

necessary for H spillover to occur is unknown, but the density of H on the promoter metal has been shown to decrease with distance from Pd.<sup>83</sup>

To enhance metal dispersion and facilitate handling and phase separation, Pd and other catalytic metals are often loaded onto support materials. Common supports for contaminant reduction (e.g.,  $\text{NO}_3^-$ ,  $\text{NO}_2^-$ ,  $\text{ClO}_4^-$ , and chlorinated organics) are activated carbon,<sup>84,85</sup> alumina,<sup>1,15,20,61,86</sup> and silica.<sup>15</sup> Other less common but effective supports for  $\text{NO}_3^-$  and  $\text{NO}_2^-$  reduction include  $\text{TiO}_2$ ,<sup>87</sup>  $\text{ZrO}_2$ ,<sup>74,85,88,89</sup>  $\text{SnO}_2$ ,<sup>89</sup> organic resins,<sup>90</sup> conducting polymers,<sup>91</sup> and carbon nanotubes.<sup>92</sup> A Au support has been shown to be effective for TCE reduction,<sup>57,58</sup> and zeolites are an effective support for reduction of chlorinated aromatics.<sup>93</sup>

Accurate characterization of supported metal catalysts is a key component of understanding reaction mechanisms and pathways. Characterization tools include nitrogen gas adsorption for surface area and pore size distribution,<sup>84</sup> CO adsorption for Pd surface area,<sup>95</sup> scanning electron microscopy (SEM) for support morphology,<sup>95</sup> transmission electron microscopy (TEM) and scanning TEM (STEM) for size and morphology of catalyst metal and/or supported nanoparticles,<sup>96,97</sup> X-ray diffraction for submicrometer particles, dynamic light scattering for micrometer particles, XPS for metal type and oxidation state, energy dispersive X-ray spectroscopy (EDX) and electron energy loss spectroscopy (EELS) for catalyst composition and/or binding state,<sup>97</sup> and high energy X-ray adsorption methods for local catalyst geometric and/or electronic structure.<sup>98–100</sup> Several publications have reviewed catalyst characterization methods,<sup>96,97,101–103</sup> and a detailed review of these methods is beyond the scope of this review. Instead, we discuss results from these methods as they apply to the focus areas of this review, i.e., reaction pathways, reaction rates, catalyst sustainability, and technology application.

Significant differences in reaction rate constants are sometimes observed when the same reactive metal is immobilized on different supports.<sup>15,73,85,104–109</sup> The catalyst support can have a direct effect on reactivity either through direct participation in catalysis or through modification of the electronic properties of the metal particles.<sup>57,106,109–111</sup> Electronic effects are most pronounced for highly dispersed metal particles with large interfacial areas,<sup>112</sup> and can influence the binding of adsorbates to particle surfaces as well as adhesion of particles to supports.<sup>113,114</sup>

The support can have an indirect effect on activity and selectivity by influencing the density, size, and morphology of catalytic metal clusters on their surface,<sup>111</sup> and thus the distribution of reactive sites. Similarly, the preparation methods influence particle morphology and composition,<sup>41</sup> and structural changes to the catalyst can occur during contaminant reduction.<sup>20,41,115</sup> The particle size determines specific surface area and relative density of high coordinated sites (e.g., terrace sites) to low coordinated sites (e.g., steps, edge, kinks) that can affect catalytic rates and mechanisms.<sup>87,116–118</sup> For example, during  $\text{NO}_2^-$  reduction on a Pd–Cu/TiO<sub>2</sub> catalyst, less N<sub>2</sub> production was observed for Pd–Cu nanoparticles <3.5 nm.<sup>87</sup> More recently, N<sub>2</sub> production from  $\text{NO}_2^-$  reduction was linearly correlated with Pd nanoparticles size when loaded on carbon nanofibers.<sup>119</sup> These trends may be related to hindered N–N pairing on smaller Pd particles that contain a high density of low coordination sites (i.e., edges and corners).<sup>85</sup> Additionally, supports with high specific surface area or microporosity can influence the activity and selectivity of reactions through mass transfer effects.<sup>108</sup>

Bimetallic systems magnify the geometric and electronic effects because the distribution of the two metals relative to each other is an important factor governing reactivity. Pd–Cu bimetallic catalysts have been synthesized as an alloy,<sup>120,121</sup> with Cu surface segregated on Pd,<sup>122</sup> and as separate Pd and Cu particles.<sup>115</sup> Batista et al.<sup>120</sup> observed similar  $\text{NO}_3^-$  reduction activities for alloyed and nonalloyed Pd–Cu catalysts, whereas Soares et al.<sup>123</sup> observed that Pd–Cu alloys were less active. The reported differences in catalyst activity as a function of catalyst structure make it difficult to develop catalyst structure–activity relationships. Interestingly, indium appears as In<sub>2</sub>O<sub>3</sub> in preparation of Pd–In catalysts,<sup>20,76</sup> but whether In<sub>2</sub>O<sub>3</sub> segregates to Pd or to the support is unclear. Results from ex situ characterization techniques (e.g., SEM, XPS, TEM) can provide detailed information regarding the size, composition, and oxidation states of bimetallic particles, but results may be misleading due to the ability of bimetallic particles to transform during reaction.<sup>20,41,115</sup> In situ experiments that are capable of characterizing catalyst structure during reactions are therefore needed to determine accurate catalyst structure–activity relationships for catalytic transformations in bimetal systems.

**2.1.1. Hydrodehalogenation.** This reaction pathway is characterized by the replacement of one or more carbon-bound halogen atoms with atomic hydrogen<sup>9,21</sup> and is relevant to all halogenated compounds, including the commonly detected groundwater contaminants TCE, PCE, and CT. For example, in aqueous solution chlorinated ethene daughter products (e.g., dichlorethene (DCE) isomers, vinyl chloride) were detected as intermediates of TCE reduction on Pd powder (Table 1), and chloroform was detected as an intermediate of CT reduction on a Pd/ $\gamma$ -Al<sub>2</sub>O<sub>3</sub> catalyst and on Pd powder (Table 1).<sup>10</sup> The basic pathways have been inferred from identification of transformation products, spectroscopic studies of the solid–gas and solid–water interface, DFT modeling, and

differences in reduction rate constants for compounds both in aqueous and gas-phase systems.<sup>124–132</sup>

The key parameters thought to affect contaminant reduction are summarized in Table 2. For reduction of chloromethanes and chloroethanes on Pd/ $\gamma$ -Al<sub>2</sub>O<sub>3</sub>, dechlorination rates were inversely proportional to calculated C–X bond strengths, e.g., increasing the number of geminal Cl atoms decreases C–Cl bond strength and results in higher reduction rates.<sup>133</sup> This same trend has been observed for gas phase reactions.<sup>125</sup> This correlation suggests that C–X bond cleavage is the rate-limiting step for the reaction and the predominant mechanism may be homolytic cleavage on the Pd catalyst,<sup>134,135</sup> indicating that adsorption strength of the halide with the catalyst is an important factor that facilitates bond cleavage.<sup>124,125,128,135,136</sup> Using XPS, Gomez-Sainero et al.<sup>137</sup> found that reduced Pd catalysts containing a residual level of unreduced Pd<sup>0</sup> exhibited higher activity for CT reduction than those that contained only metallic or unreduced Pd. These Pd<sup>0</sup> species are proposed initial products of CT dechlorination. Aqueous phase studies indicate that carbon–carbon coupling can also occur during hydrodehalogenation.<sup>10</sup> Ethane, and minor amounts of ethene, propane, and propene were observed during CT reduction using a Pd/ $\gamma$ -Al<sub>2</sub>O<sub>3</sub> catalyst (Table 1).<sup>10</sup> This observation was attributed to the formation of adsorbed trichloromethyl radicals during reduction.

Hydrodehalogenation mechanisms of halogenated alkenes do not appear as straightforward as those of halogenated alkanes. Mackenzie et al.<sup>133</sup> reported that dehalogenation rates increased with increasing C–X bond strength and decreasing number of geminal Cl atoms; they attributed this observation to hydrogenation of the C=C bond before C–X bond scission, and postulated that the former was rate-limiting (Table 2).<sup>133</sup> DFT studies indicate that the most energetically favorable adsorption configuration for chlorinated ethenes on Pd is through a C=C di- $\sigma$  bond, and the adsorption strength increases with decreasing number of Cl atoms.<sup>127,138,139</sup> Therefore, it is possible that increasing adsorption strength corresponds to greater reaction rate constants.<sup>133</sup> Although C=C di- $\sigma$  bonding of chlorinated ethenes to Pd is most energetically favorable, DFT studies<sup>127,138,139</sup> and in situ surface-enhanced Raman spectroscopy (SERS)<sup>132</sup> results indicate that the Cl atoms in chlorinated ethenes also adsorb to the catalyst surface. For the case of 1,1-DCE, experimental evidence suggests that C=C di- $\sigma$  bonding to Pd/Au is followed by dissociative adsorption of the C–Cl bonds to form an adsorbed vinylidene intermediate followed by hydrogenation of the C=C bond.<sup>132</sup> Further studies are clearly needed to elucidate these catalytic mechanisms.

In general, ethane is observed as the primary product from aqueous-phase TCE and PCE reduction on a Pd/ $\gamma$ -Al<sub>2</sub>O<sub>3</sub> catalyst,<sup>9,10,131</sup> (Table 1). Both gas- and aqueous-phase studies indicate that hydrogenation of unsaturated carbon–carbon bonds can occur during hydrodehalogenation, but in the aqueous phase dehalogenation products are more favorable than hydrogenation products.<sup>129</sup> For example, the hydrogenation of vinyl chloride forms primarily ethane and ethyl chloride in the aqueous and gas phases, respectively.<sup>129</sup> Studies have detected traces of C<sub>4</sub> compounds during catalytic reduction of 1,1-DCE, which were attributed to adsorbed vinylidene polymerization.<sup>132</sup> Nuclear magnetic resonance (NMR) studies of gas-phase TCE reduction on a Pd/ $\gamma$ -Al<sub>2</sub>O<sub>3</sub> catalyst indicate C=C bond cleavage occurs,<sup>131</sup> which also could result in polymerization reactions.

Table 2. Factors Affecting Catalytic Reduction Rates on Pd–M Catalysts

contaminant	promoter (M)	bond broken	reaction	bond strength of bond broken (kJ/mol)	effect of bond strength	effect of pH
oxyanions						
NO <sub>3</sub> <sup>−</sup>	Cu, In, Sn	N–O	NO <sub>3</sub> <sup>−</sup> → NO <sub>2</sub> + O <sup>−</sup>	263 <sup>a</sup>	difficult to assess due to different acitve sites	strong effect, acidic needed
NO <sub>2</sub> <sup>−</sup>		N–O	NO <sub>2</sub> <sup>−</sup> → NO <sub>2</sub> + O <sup>−</sup>	217 <sup>a</sup>		
BrO <sub>3</sub> <sup>−</sup>		Br–O	BrO <sub>3</sub> <sup>−</sup> → BrO <sub>2</sub> + O <sup>−</sup>	242 <sup>a</sup>		
ClO <sub>3</sub> <sup>−</sup>		Cl–O	ClO <sub>3</sub> <sup>−</sup> → ClO <sub>2</sub> + O <sup>−</sup>	201 <sup>a</sup>		
ClO <sub>4</sub> <sup>−</sup>	Re	Cl–O	ClO <sub>4</sub> <sup>−</sup> → ClO <sub>3</sub> + O <sup>−</sup>	197 <sup>aa</sup>		
nitrosamines						
(C <sub>6</sub> H <sub>5</sub> ) <sub>2</sub> N–NO		N–N	R <sub>2</sub> N – NO → R <sub>2</sub> N <sup>•</sup> + NO	95 <sup>b</sup>	no	none
chlorinated alkanes						
CCl <sub>4</sub>		C–Cl	CCl <sub>4</sub> + <sup>•</sup> CCl <sub>3</sub> + Cl	297 <sup>b</sup>	yes, strongly	strong effect, basic needed
CHCl <sub>3</sub>		C–Cl	CHCl <sub>3</sub> → <sup>•</sup> CHCl <sub>2</sub> + Cl	311 <sup>b</sup>		
CH <sub>2</sub> Cl <sub>2</sub>		C–Cl	CH <sub>2</sub> Cl <sub>2</sub> → <sup>•</sup> CH <sub>2</sub> Cl + Cl	338 <sup>b</sup>		
chlorinated alkenes						
C <sub>2</sub> Cl <sub>4</sub>		C–Cl	C <sub>2</sub> Cl <sub>4</sub> → <sup>•</sup> C <sub>2</sub> Cl <sub>3</sub> + Cl	387 <sup>b</sup>	no	strong effect, basic needed
C <sub>2</sub> HCl <sub>3</sub>		C–Cl	C <sub>2</sub> HCl <sub>3</sub> → <sup>•</sup> C <sub>2</sub> HCl <sub>2</sub> + Cl	392 <sup>c</sup>		
C <sub>2</sub> H <sub>2</sub> Cl <sub>2</sub>		C–Cl	C <sub>2</sub> H <sub>2</sub> Cl <sub>2</sub> → <sup>•</sup> C <sub>2</sub> H <sub>2</sub> Cl + Cl	394 <sup>c</sup>		
C <sub>2</sub> H <sub>3</sub> Cl		C–Cl	C <sub>2</sub> H <sub>3</sub> Cl → <sup>•</sup> C <sub>2</sub> H <sub>3</sub> + Cl	352 <sup>d</sup>		
halogenated aromatics						
C <sub>6</sub> H <sub>5</sub> I		C–I	C <sub>6</sub> H <sub>5</sub> I → <sup>•</sup> C <sub>6</sub> H <sub>5</sub> + I	272 <sup>b</sup>	yes, strongly	strong effect, basic needed
C <sub>6</sub> H <sub>5</sub> Br		C–Br	C <sub>6</sub> H <sub>5</sub> Br → <sup>•</sup> C <sub>6</sub> H <sub>6</sub> + Br	336 <sup>b</sup>		
C <sub>6</sub> H <sub>5</sub> Cl		C–Cl	C <sub>6</sub> H <sub>5</sub> Cl → <sup>•</sup> C <sub>6</sub> H <sub>5</sub> + Cl	400 <sup>b</sup>		
C <sub>6</sub> H <sub>5</sub> F		C–F	C <sub>6</sub> H <sub>5</sub> F → <sup>•</sup> C <sub>6</sub> H <sub>5</sub> + F	526 <sup>b</sup>		

<sup>a</sup>Bond strength calculated using listed reaction and enthalpies of formation. Details are provided in the Supporting Information. <sup>b</sup>Ref 208. <sup>c</sup>Ref 209. <sup>d</sup>Ref 210.

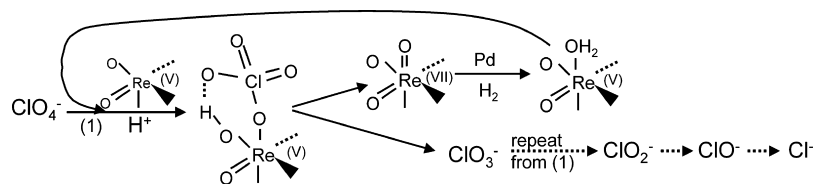
The dehalogenation rates of halogenated benzenes depend weakly on halogen substituents, increasing according to I > Br > Cl > F.<sup>133</sup> C–X bond scission may be the rate-limiting step for dehalogenation of these compounds, but the nature of the catalyst can alter this dependence. A different order of reactivity (i.e., Br > Cl > I > F) was found for a Pd catalyst supported on a 20:80 mixture of aluminum orthophosphate,<sup>140</sup> suggesting that the halogen substituent(s) may determine the adsorption strength and bonding configuration of the aromatic to the catalyst surface. Hydrogenation of aromatic rings may occur, but this appears to be less favorable than aromatic dehalogenation in water.<sup>13,70</sup>

Halogenated aromatic compounds other than halogenated benzenes have been evaluated for Pd-based catalytic reduction, including chlorinated phenols, biphenyls, pesticides (i.e., DDT), and antimicrobials (i.e., dichlorophenol).<sup>141–145</sup> Among these, chlorinated phenols are the most widely studied, and activity for their reduction over Pd generally decreases with increasing substitution.<sup>14,146</sup> As above, this suggests adsorption and not C–Cl bond cleavage is rate-determining. Aqueous-phase reduction for the variety of halogenated aromatic compounds evaluated generally proceeds via sequential dechlorination.<sup>145</sup> When multiple halogens are present, results from 2,4-dichlorophenol reduction suggest that less sterically hindered halogens are removed first.<sup>147</sup> When H<sub>2</sub> is the electron donor, aromatic ring hydrogenation has been observed to occur after dehalogenation.<sup>147</sup> Both cyclohexanone<sup>144,148</sup> and cyclohexanol<sup>143,147</sup>

have been observed, suggesting oxidation of the hydroxyl group during ring hydrogenation and subsequent reduction back to the alcohol.

Recent work on the hydrogenolysis of hydrocarbons on Pt group metals indicates that reaction rate constants are related to adsorption strength, which further depends on the metal facet on which the sites are located.<sup>149</sup> This conclusion appears to translate to hydrodehalogenation reactions. For halogenated alkanes and aromatics, where the rate-limiting step is thought to be C–X bond cleavage,<sup>133</sup> experiments in both gas- and liquid-phase show that hydrodechlorination rate constants (catalyst mass-normalized) increase with increasing Pd particle size.<sup>116–118</sup> Larger particles have a higher proportion of high coordinated metal sites. By contrast, experiments show enhanced TCE reduction rate constants on nanoparticle (NP) catalysts,<sup>55,57,58</sup> which have a higher proportion of low coordinated metal sites. This finding is consistent with recent DFT calculations showing TCE adsorbs more strongly on Pd clusters than on a Pd(111) plane.<sup>127</sup> TCE reduction is also enhanced when Pd is supported by a second metal,<sup>55,57,58</sup> apparently due to stronger adsorption on the bimetallic particle relative to Pd alone.<sup>127,138,139,150–153</sup>

**2.1.2. Hydrodeoxygenation.** This reaction pathway is characterized by the sequential removal of oxygen atoms from oxyanions by hydrogenation to water. Oxygen atom transfer (OAT) from the oxyanion to the catalyst metal lowers the redox state of the contaminant. The roles of Pd for monometallic catalysts are to (1) dissociate H<sub>2</sub> and (2) facilitate H<sub>2</sub>O formation

Scheme 1. Perchlorate Reduction on Pd/Re.<sup>4</sup>

from abstracted oxygen atoms. Key examples of contaminants reduced on monometallic Pd are  $\text{NO}_2^-$ ,  $\text{BrO}_3^-$ , and  $\text{ClO}_3^-$ .<sup>2,6,73,154,155</sup> The roles of Pd for bimetallic catalysts are to (1) dissociate  $\text{H}_2$  and (2) reduce the catalyst metal-oxo species generated upon OAT from the contaminant. Important examples are  $\text{NO}_3^-$  and  $\text{ClO}_4^-$ . The proposed mechanism is illustrated for the reduction of  $\text{ClO}_4^-$  on Re in Scheme 1.<sup>4</sup> XPS results indicate that the Re promoter metal cycles between the +7 oxidation state and lower oxidation states (+5/+4 and +1) to promote reduction through OAT.<sup>84</sup> A key step in this process is thought to be hydrogen-bonding between an oxygen atom in  $\text{ClO}_4^-$  and a hydrogen atom on the protonated surface-bound  $\text{ReOOH}$  complex.<sup>4</sup> As a result, activity for  $\text{ClO}_4^-$  reduction increases with decreasing pH. Although OAT mechanisms are thought to be applicable to a wide range of oxyanion contaminants, experimental evidence suggests that the active site differs among oxyanions. For example,  $\text{NO}_3^-$  requires Pd–M bimetallic catalysts, where M = Cu, In, Sn,<sup>1,15,75,87,89,121,122,156,157</sup> and  $\text{ClO}_4^-$  is reduced on Pd–Re catalysts.<sup>3–6</sup> Although  $\text{NO}_2^-$ ,  $\text{BrO}_3^-$ , and  $\text{ClO}_3^-$  can be reduced on Pd monometallic catalysts, rate enhancements relative to Pd have been observed for these contaminants on Pd–M catalysts, where M = Cu, In, and Re, respectively,<sup>3,6,121</sup> suggesting they can also be reduced by the OAT mechanism. The rate enhancement on Pd–M relative to Pd only catalysts is likely due to the higher oxophilicity of the promoter metals.<sup>121</sup>

Relating atomic structure of oxyanion contaminants to reduction rate constants is difficult due to the need for different catalysts for different contaminants. If reactivity were governed solely by X–O bond strength, the rate would decrease in the order  $\text{ClO}_4^- > \text{ClO}_3^- > \text{NO}_2^- > \text{BrO}_3^- > \text{NO}_3^-$  (Table 2). Work by Abu-Omar et al.<sup>158</sup> investigating OAT using homogeneous methylrhodium oxide catalysts reported rates decreasing as  $\text{BrO}_3^- > \text{ClO}_3^- > \text{NO}_3^- > \text{ClO}_4^-$ , which indicates that factors other than bond strength govern reactivity.

Recent work with Pd–Re/C catalysts showed the electronic environment of the Re promoter metal active site could increase the  $\text{ClO}_4^-$  reduction rate constant.<sup>5,6</sup> Preparation of Pd–Re/C catalysts using a  $[\text{ReO}_2(\text{py-X})_4]\text{Cl}$  salt (py-X = 4-substituted pyridine; X = H, Me, OMe, NMe<sub>2</sub>) yielded reduction rate constants up to 5 times greater than Pd–Re/C catalysts prepared from  $\text{NH}_4\text{ReO}_4$ .<sup>4</sup> Perchlorate reduction rate constants increased based on the increasing donor character of the pyridine ligand ( $\text{H} < \text{Me} < \text{OMe} < \text{NMe}_2$ ). Additional work showed a 20-fold rate constant enhancement using a chlorobis-(2-(2'-hydroxyphenyl)-2-oxazoline)-oxorhenium(V) precursor compared to  $\text{NH}_4\text{ReO}_4$ .<sup>6</sup> These studies illustrate the importance of engineering active sites for contaminant reduction, and this work may also translate to enhanced reduction rates for other oxyanions.

**2.1.2.1. Oxyanion Selectivity.** Reduction of halogen oxyanions (e.g.,  $\text{ClO}_4^-$ ,  $\text{BrO}_3^-$ ) leads to  $\text{X}^-$  as the final product and selectivity is not a consideration, in contrast to  $\text{NO}_3^-$  and  $\text{NO}_2^-$ , where the final products are either  $\text{N}_2$  or  $\text{NH}_4^+$ .

Ammonium is of environmental concern because drinking water standards have been set at 0.5 mg/L by the World Health Organization.<sup>159</sup> Product selectivity for  $\text{NO}_3^-$  and  $\text{NO}_2^-$  is primarily a function of the catalyst structure and solution conditions. The exact pathways for  $\text{N}_2$  and  $\text{NH}_4^+$  formation are still debated in the literature. A number of studies suggest that the rate-limiting steps for formation of  $\text{N}_2$  and  $\text{NH}_4^+$  products involve either dimerization or hydrogenation of the NO intermediate, respectively.<sup>62,85</sup> Insights were obtained from studies of electrochemical reduction of NO over Pt and Pd electrodes.<sup>160–162</sup> In these studies, reduction of adsorbed NO to HNO leads to  $\text{NH}_4^+$ , while reaction of adsorbed NO with solution-phase NO leads to an  $\text{HN}_2\text{O}_2$  intermediate, and ultimately  $\text{N}_2\text{O}$  and  $\text{N}_2$ . Results from other studies using attenuated total reflection (ATR) infrared vibrational spectroscopy indicate that while NO dimerization may be responsible for  $\text{N}_2$ , hydrogenation of adsorbed  $\text{HNO}_2^-$  is responsible for the formation of  $\text{NH}_4^+$ .<sup>154,155</sup>

There is evidence that catalyst structure has a substantial influence on selectivity of  $\text{N}_2$  over  $\text{NH}_4^+$ . Studies suggest that  $\text{N}_2$  formation is enhanced at high-coordinated and  $\text{NH}_4^+$  formation is enhanced at low-coordinated metal sites, respectively.<sup>85,119,163</sup> Poisoning of low-coordinated Pd sites with Bi has been shown to decrease  $\text{NH}_4^+$  production during  $\text{NO}_2^-$  reduction.<sup>163</sup>

Solution conditions also affect selectivity for  $\text{NH}_4^+$  versus  $\text{N}_2$ . During  $\text{NO}_3^-$  reduction, the selectivity for  $\text{NH}_4^+$  over  $\text{N}_2$  increases with increasing pH.<sup>62,74</sup> Higher pH (relative to the  $\text{pH}_{\text{zpc}}$ ) corresponds to a more negative surface charge, and the electrostatic repulsion of  $\text{NO}_3^-$  and  $\text{NO}_2^-$  ions creates a catalyst surface with a high H:N species surface coverage and promotes the production of  $\text{NH}_4^+$ .<sup>62</sup> Additionally, the adsorption of  $\text{OH}^-$  ions to reaction sites may inhibit the pairing of nitrogen species, resulting in increased  $\text{NH}_4^+$  production over  $\text{N}_2$ .<sup>62</sup> Also, higher initial  $\text{NO}_3^-$  concentration favors selectivity for  $\text{N}_2$  over  $\text{NH}_4^+$  due to the higher surface coverage of N-species and the greater chance for N–N pairing.<sup>62</sup> Studies have also shown that higher  $\text{HCO}_3^-$  concentration results in higher selectivity of  $\text{NH}_4^+$  over  $\text{N}_2$ , which was attributed to lower adsorption of  $\text{NO}_3^-$  in the presence of  $\text{HCO}_3^-$ , leading to a high H:N species surface coverage.<sup>164</sup>

**2.1.3. N–N Hydrogenolysis.** This reaction pathway is relevant to the reduction of N-nitrosamines (Table 1). For NDMA, DFT calculations indicate that both upright adsorption of adjacent O–N atoms and flat adsorption of adjacent O–N–N atoms on Pd(111) are possible.<sup>165</sup> N–N bond cleavage yields two separate surface fragments, dimethylamine ( $\text{N}(\text{CH}_3)_{2(\text{ad})}$ ) and nitric oxide ( $\text{NO}_{(\text{ad})}$ ). The former subsequently desorbs and the latter can be further reduced to  $\text{NH}_4^+$  or  $\text{N}_2$ .<sup>7,8,165</sup> The factors affecting the distribution of  $\text{NH}_4^+$  and  $\text{N}_2$  have not been identified for NDMA reduction.

Azo dye contaminants are reduced via a similar reaction pathway over Pd. First, the  $\text{N}=\text{N}$  group is reduced to  $\text{N}=\text{N}$ , and then N–N bond cleavage occurs to yield aromatic amine

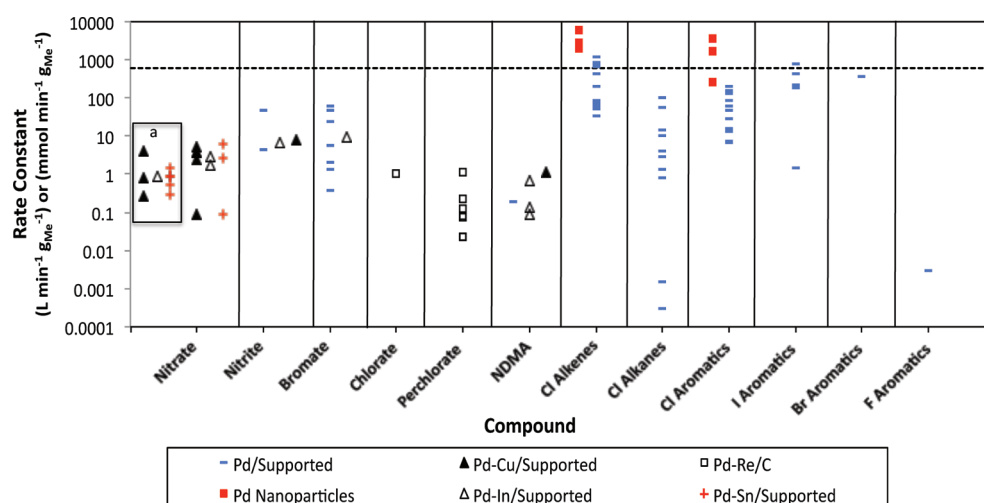


**Figure 2.** Catalytic rate constants for a variety of contaminants from batch reactors using Pd-based catalysts and  $\text{H}_2$  in water. Rates contained within the box labeled “a” are given in units of  $\text{mmol min}^{-1} \text{g}_{\text{Me}}^{-1}$ . Dashed line represents an estimate of the mass transfer rate ( $k_{\text{m,norm}}$ ) in a hypothetical fixed-bed reactor operation. Values for rate constants were obtained from various studies, with a temperature range of 10–30 °C. Reaction conditions are given in the Supporting Information (Table S-2).

products.<sup>166</sup> For example, reduction of Sunset Yellow FCF dye over a Mg/Pd catalysts yielded sulfanilic acid.<sup>167</sup>

As opposed to N–N bond cleavage, DFT calculations indicate N–O bond cleavage can also be energetically favorable for N-nitrosamines.<sup>165</sup> Ranea et al.<sup>165</sup> used DFT-calculated transition states to show that N–N dissociation kinetics of NDMA are 20 orders of magnitude faster than N–O dissociation at room temperature over a Pd catalyst. The kinetics of these two pathways were found to be comparable over a Ni surface. However, dimethylamine has been observed as a reduction product for Raney-Ni<sup>27</sup> and NiB<sup>28</sup> catalysts, suggesting that N–O bond cleavage is not an important mechanism at room temperature.

**2.2. Rate Constants for Contaminant Reduction.** First- and zeroth-order rate constants for contaminant reduction in deionized water for a variety of contaminants and Pd-based catalysts are summarized in Figure 2 and specific values for reaction conditions and rate constants are provided in the Supporting Information (Table S-2). Rate constants shown are normalized to total catalyst metal loading by weight (Me), and are indicative of batch systems where external diffusion limitations have been eliminated. Also shown in Figure 2 (dashed line) is an estimate of the mass-transfer rate of contaminants to the catalyst surface in a typical packed-bed flow-through reactor. This estimate was determined by using the Frossling correlation for the pure diffusion case,<sup>168</sup> and does not consider internal mass-transfer limitations that may occur within inner catalyst pores. The liquid to solid mass-transfer rate ( $k_{\text{m}}$  ( $\text{cm s}^{-1}$ )) to the catalyst surface is expressed as

$$k_{\text{m}} = \frac{D_{\text{w}}}{r_{\text{p}}} \quad (3)$$

where  $D_{\text{w}}$  is the approximate diffusion coefficient of contaminants in water ( $1 \times 10^{-5} \text{ cm}^2 \text{ s}^{-1}$ ),<sup>169</sup> and  $r_{\text{p}}$  is the catalyst particle radius (0.1 cm). These values were chosen to represent typical contaminants and conditions in large-scale flow-through reactors. To ensure that eq 3 is appropriate to determine  $k_{\text{m}}$ , the Peclet Number was calculated based on the flow conditions in a field-scale catalytic reactor study.<sup>170</sup> The Peclet Number was  $\gg 1$ , indicating that eq 3 is valid. The value for  $k_{\text{m}}$  was converted

to a normalized mass transfer rate ( $k_{\text{m,norm}}$ ) to provide units of  $\text{L min}^{-1} \text{g}_{\text{Me}}^{-1}$ , by using a 1.0 wt % Pd loading and a  $100 \text{ m}^2 \text{g}_{\text{cat}}^{-1}$  surface area, yielding a value of  $k_{\text{m,norm}} = 600 \text{ L min}^{-1} \text{g}_{\text{Me}}^{-1}$ .

Measured rate constants for most contaminants are lower than the estimated  $k_{\text{m,norm}}$  described above, indicating that research on applied catalytic technologies should be focused on increasing intrinsic reaction rates. Notable exceptions include dichloroethene and vinyl chloride on Pd/ $\gamma\text{-Al}_2\text{O}_3$ ,<sup>133</sup> diatrizoate on Pd/ $\gamma\text{-Al}_2\text{O}_3$ ,<sup>171</sup> and chlorobenzene<sup>55</sup> and TCE<sup>55,58</sup> on nanoparticle catalysts, whose measured rate constants are approximately equal to or higher than  $k_{\text{m,norm}}$  (see Figure 2).

In general, measured reaction rate constants are highest for chlorinated alkenes and halogenated aromatics, with the exception of fluorinated aromatics. Dehalogenation rate constants of partially chlorinated alkanes are orders of magnitude lower than those of chlorinated alkenes and aromatics. The assessment of oxyanion reduction rates is complicated by the fact that different catalysts are needed for different oxyanions. In general,  $\text{NO}_2^-$  and  $\text{BrO}_3^-$  reduction rates on Pd are faster than those of  $\text{NO}_3^-$  and  $\text{ClO}_3^-$  on Pd-M catalysts. Perchlorate reduction rates vary by approximately 2 orders of magnitude.<sup>4–6</sup> Measured rate constants for oxyanions are strongly affected by surface charge of the supported catalyst. At pH values above the  $\text{pH}_{\text{pzc}}$  of the supported catalyst surface, the negatively charged oxyanions are repelled by the negatively charged support leading to a drop in reduction rate constants.<sup>73,89,107,172</sup>

Measured activation energies are useful for determining the effect of temperature on contaminant reduction rates. However, few studies report activation energies for catalytic reduction of contaminants in water. The activation energies for  $\text{NO}_3^-$ , 4-chlorophenol, and 2,4-dichlorophenol have been measured and are 4.2–47 kJ/mol,<sup>61,173</sup> 85.8 kJ/mol,<sup>144</sup> and 45–55.8 kJ/mol,<sup>147,174</sup> respectively.

**2.3. Long-Term Sustainability.** **2.3.1. Catalyst Inhibition and Fouling.** Numerous studies report inhibition and/or fouling of Pd-based catalysts by natural water constituents, including sulfide and other low molecular weight inorganic solutes,<sup>76,86,175,176</sup> redox active metals,<sup>177</sup> dissolved organic matter (DOM),<sup>86,171,178</sup> microbial biomass,<sup>179</sup> and mineral precipitates.<sup>179</sup> Reduced sulfur species (i.e.,  $\text{HS}^-$  and  $\text{SO}_3^{2-}$ ) are

the primary low molecular weight inorganic solutes that foul Pd-based catalysts. Reduced sulfur forms strong complexes with Pd and other catalyst metals,<sup>180</sup> which blocks reaction sites and prevents compound transformations.<sup>76,86,175,176,181</sup> Studies have shown that fouling can occur at low solute levels (0.06 mmol S/g supported catalyst) and oxidative regeneration is necessary to remove the bound sulfur.<sup>76,176</sup> XPS measurements indicate that PdS and In<sub>2</sub>S<sub>3</sub> compounds form on catalyst surfaces following exposure to aqueous HS<sup>-</sup>.<sup>76</sup> Other anions that bind to Pd sites include high levels of halide ions, HCO<sub>3</sub><sup>-</sup>, SO<sub>4</sub><sup>2-</sup>, and OH<sup>-</sup>, which form weak interactions with the catalyst metals and inhibition is usually reversible upon rinsing catalysts with deionized water.<sup>86,157,182</sup> The anions mentioned above have shown varying affinities for catalysts comprising different catalyst formulations.<sup>4,86,157,182</sup> For example, NO<sub>3</sub><sup>-</sup> reduction using a Pd-Cu/ $\gamma$ -Al<sub>2</sub>O<sub>3</sub> catalyst was almost completely inhibited in the presence of 1000 mg/L Cl<sup>-</sup>,<sup>86</sup> while no effect was observed during ClO<sub>4</sub><sup>-</sup> reduction in the presence of 1000 mg/L Cl<sup>-</sup> using a Re-Pd/C catalyst.<sup>4</sup> The results can be attributed to an enhanced physical and/or chemical adsorption of Cl<sup>-</sup> to Cu.<sup>183</sup>

Hydrodehalogenation reactions can lead to self-inhibition due to release of halide acids produced during the reduction process, which can foul the Pd catalyst if allowed to build up to high levels (e.g., 700–2000 mol HCl/mol Pd),<sup>70,72,147,148,184,185</sup> while lower levels showed no effect (213 mol HCl/mol Pd).<sup>186</sup> The mechanism of catalyst fouling during the reduction of TCE by Pd/C catalysts was attributed to the production of H<sup>+</sup> and Cl<sup>-</sup> at the catalyst surface.<sup>184</sup> The high Cl<sup>-</sup> concentration and low pH possibly stabilize Pd<sup>2+</sup> on the catalyst surface by the formation of PdCl<sub>3</sub><sup>-</sup> and PdCl<sub>4</sub><sup>2-</sup> species.<sup>187</sup> As discussed in Section 2.1, the Pd<sup>n+</sup> species may be important intermediates in the reduction of halogenated organics.<sup>137</sup> The solubility of PdCl<sub>3</sub><sup>-</sup> and PdCl<sub>4</sub><sup>2-</sup> species in 0.1 M KCl has been reported to increase by 4 orders of magnitude when the pH is lowered from 7 to 4.<sup>188</sup> Therefore, high pH or the presence of a pH buffer can limit catalyst deactivation,<sup>184</sup> as long as the pH buffer does not result in catalyst fouling. The above mechanism is thought to be applicable for other halogens (i.e., Br<sup>-</sup>, I<sup>-</sup>, F<sup>-</sup>), but solubility data are limited for Pd-X species.<sup>189</sup> However, Mackenzie et al.<sup>133</sup> observed that the addition of Br<sup>-</sup> and I<sup>-</sup> ions to batch reactions inhibited dehalogenation rates of halogenated organics, supporting the mechanism discussed above.

The presence of redox active metals in water can also lead to catalyst fouling.<sup>177</sup> Hildebrand et al.<sup>177</sup> reported that Cu<sup>2+</sup> (80  $\mu$ M), Pb<sup>2+</sup> (0.5  $\mu$ M), Sn<sup>2+</sup> (40  $\mu$ M), and Hg<sup>2+</sup> (0.5  $\mu$ M) decreased rate constants of TCE reduction on Pd/Fe<sub>2</sub>O<sub>3</sub> NPs by 97.0, 76.0, 99.8, and 98.0%, respectively, compared to rate constants measured in deionized water. The mechanism of catalyst fouling was not addressed, but is likely a result of a redox reaction between the metal ions and Pd-H<sub>ads</sub>, resulting in reduction of the metal cations to their zerovalent states and subsequent blockage of active sites.

DOM is ubiquitous in natural waters and has been shown to cause catalyst fouling in several studies.<sup>86,171,178</sup> For example, it has been shown that the rate constants of NO<sub>3</sub><sup>-</sup> reduction (Pd-Cu/ $\gamma$ -Al<sub>2</sub>O<sub>3</sub> catalyst) decreased 84 and 97% relative to deionized water in the presence of 3.3 mg C/L of humic acid and 2.88 mg C/L of DOM present in natural groundwater, respectively.<sup>86</sup> Likewise, the reduction rate of iodinated X-ray contrast agents on Pd/ $\gamma$ -Al<sub>2</sub>O<sub>3</sub> catalysts decreased by ~75% relative to deionized water in the presence of 5 mg C/L of DOM.<sup>171</sup> In both studies, pretreatment of the water with

activated carbon to remove DOM prior to catalytic reduction significantly eliminated inhibitory effects. Fundamental work investigating the mechanisms of catalyst fouling by DOM and characterization of the portion of DOM that fouls catalysts has not been performed.

The fouling of catalysts by microbial biomass has not been observed in most lab scale studies due to the relatively short operation time of most experiments and the slow growth of bacteria under anaerobic conditions. However, in long-term lab and pilot studies that treated natural waters, microbial fouling has been shown to affect catalyst performance.<sup>175,179,190</sup> Under anaerobic conditions a variety of autotrophic bacteria (e.g., pseudomonas, aeromonas) are able to grow utilizing H<sub>2</sub> as the electron donor, CO<sub>2</sub> as the carbon source, and either the target contaminant or SO<sub>4</sub><sup>2-</sup> as the terminal electron acceptor. In SO<sub>4</sub><sup>2-</sup> free waters, the growth of biomass has been shown to increase rates of NO<sub>3</sub><sup>-</sup> reduction.<sup>179</sup> In SO<sub>4</sub><sup>2-</sup> containing waters, microbial reduction leads to production of HS<sup>-</sup>, a strong catalyst poison.<sup>175,190</sup> For this reason, catalytic field studies use periodic disinfectant treatment (e.g., OCl<sup>-</sup>, H<sub>2</sub>O<sub>2</sub>) to control microbial growth and oxidize deactivated PdS surface sites.<sup>170,191,192</sup> Details of field studies are provided in Section 2.4.

Mineral precipitation on the catalyst surface can result in blockage of active sites and lead to decreases in contaminant reduction rate constants. Mineral precipitation by hardness ions (e.g., Ca<sup>2+</sup> and Mg<sup>2+</sup>) does not occur to a large extent during catalytic dehalogenation,<sup>178</sup> likely due to the generation of H<sup>+</sup> during reaction. However, mineral precipitation has been suggested to foul Pd-based catalysts during catalytic NO<sub>3</sub><sup>-</sup> reduction,<sup>179,193</sup> which is likely due to the generation of OH<sup>-</sup> during the NO<sub>2</sub><sup>-</sup> reduction step.

**2.3.2. Fouling Resistant Catalysts.** Because fouling has been recognized as one of the primary challenges associated with the application of Pd-based catalytic treatment technologies, studies have focused on designing fouling resistant catalysts.<sup>93,178,194,195</sup> Attempts include the use of zeolite supports,<sup>93,192</sup> incorporation of active metals into polymers,<sup>178,194</sup> and synthesis of core-shell catalyst NPs.<sup>195</sup>

The use of zeolites as supports has proven to be a successful method to mitigate catalyst fouling by sulfite. Schüth et al.<sup>93</sup> tested a Pd catalyst supported on zeolites for the reduction of 1,2-dichlorobenzene (1,2-DCB) in the presence of aqueous sulfite. It was found that the optimal support was a hydrophobic zeolite Y with a 0.74 nm pore diameter. The zeolite structure prevented fouling of internally located Pd sites by excluding sulfite based on both molecular size and hydrophobicity. The Pd/zeolite Y catalyst showed sustained reduction of chlorinated hydrocarbons for a period of over 2 years at a groundwater site with periodic regeneration.<sup>192</sup>

The use of hydrophobic silicone polymers, in either thin membrane composites incorporating the active Pd catalyst<sup>194</sup> or encapsulating Pd/ $\gamma$ -Al<sub>2</sub>O<sub>3</sub> catalysts particles,<sup>178</sup> has shown resistance to catalyst fouling. Work performed by Kopinke et al.<sup>178</sup> showed that the reduction rate constant of chlorobenzene with a Pd/ $\gamma$ -Al<sub>2</sub>O<sub>3</sub> catalyst significantly decreased in the presence of a soil slurry supernatant (40 mg/L DOM). However, coating the catalyst with hydrophobic silicone polymers was able to protect the Pd catalyst against sulfite and DOM fouling for at least 24 h.

Changing the electronic structure of Pd also has been reported to limit sulfide fouling. Synthesized Pd/Au NPs were reported to have a resistance to sulfide fouling.<sup>195</sup> This observation was attributed to the electronic interaction between

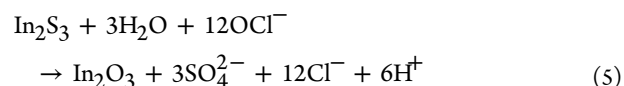
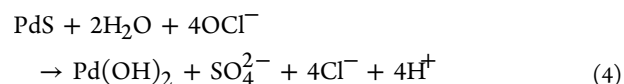
Pd–Au, and not due to Au acting as a sulfide sink.<sup>195</sup> Published data indicate that Pd–S is more energetically favorable than Au<sub>2</sub>S.<sup>180</sup> X-ray absorption spectroscopy (XAS) indicates that Pd–Au NPs supported on C are more resistant to oxidation by oxygen relative to C-supported Pd NPs,<sup>196</sup> but XPS and XAS measurements of these catalysts after sulfide fouling have not been performed.

**2.3.3. Regeneration Strategies.** Regeneration strategies for sulfur-fouled catalysts employ catalyst treatment with a strong oxidant, including HOCl/OCl<sup>−</sup>,<sup>76,86,175,176,197</sup> H<sub>2</sub>O<sub>2</sub>,<sup>76,176,192</sup> KMnO<sub>4</sub>,<sup>198,199</sup> dissolved oxygen,<sup>76,176</sup> and air exposure (for dried catalysts).<sup>200</sup> S-fouled catalysts are not easily regenerated due to the (1) strong bonding interaction between S<sup>2−</sup> and catalytic metals,<sup>180</sup> (2) ability of sulfide to diffuse into bulk Pd<sup>201</sup> creating a reservoir for surface fouling, and (3) fouling of inner catalyst pores preventing access of oxidants. The regeneration of fouled catalysts is influenced by the foulant species, concentration of the oxidant at the catalyst surface, regeneration time, solution pH, and supported catalyst used.

The concentration of the oxidant at the catalyst surface is perhaps the most important parameter governing regeneration efficiency, which is influenced by the oxidant reactivity, electrostatics between the oxidant and the catalyst surface, and solution pH. Highly reactive oxidants, such as H<sub>2</sub>O<sub>2</sub>, have high redox potentials, but have shown mixed results as a regenerant. The regeneration of sulfide-fouled Pd/γ-Al<sub>2</sub>O<sub>3</sub> catalysts with H<sub>2</sub>O<sub>2</sub> was ineffective at restoring catalyst activity,<sup>76,176,198</sup> possibly due to consumption of H<sub>2</sub>O<sub>2</sub> in side-reactions before it gained access to fouled catalytic sites. By contrast, the regeneration of sulfide-fouled Pd/zeolite Y catalysts with H<sub>2</sub>O<sub>2</sub> was effective at restoring catalyst activity,<sup>192</sup> and may be related to the zeolite structure that prevented fouling of inner catalyst reactive sites. It has been reported that H<sub>2</sub>O<sub>2</sub> decomposes rapidly in the presence of Pd to form short-lived hydroxyl radicals,<sup>202</sup> which may have a beneficial effect on catalyst regeneration, but hydroxyl radicals may not be effective at regenerating inner catalyst pores. DO is not effective at regenerating S-fouled catalysts, as it rapidly dissociates on Pd and reacts with Pd–H to form water.<sup>203</sup> By contrast HOCl/OCl<sup>−</sup> and MnO<sub>4</sub><sup>−</sup> have shown the best results as regenerants, as they are stable enough in water to reach fouled catalytic sites located in inner catalyst pores. Electrostatic interactions are also important for the oxidant to gain access to these sites. Low pH conditions result in a positively charged catalyst surface, which has been shown to improve the efficiency of anionic oxidants such as MnO<sub>4</sub><sup>−</sup>.<sup>198</sup>

Another key parameter for catalyst regeneration is stability of the supported Pd and promoter metal phases, which is a function of the supported catalyst composition, solution pH, and oxidant used. Regeneration of S-fouled Pd–Cu/γ-Al<sub>2</sub>O<sub>3</sub> catalysts with HOCl/OCl<sup>−</sup> resulted in significant dissolution of Cu.<sup>76,86</sup> Partial regeneration of S-fouled Pd–In/γ-Al<sub>2</sub>O<sub>3</sub> catalysts in batch reactors (39–60% of initial rate constants for NO<sub>3</sub><sup>−</sup> reduction) was achievable with 56 mM HOCl/OCl<sup>−</sup> solutions and the Pd and In contents were stable.<sup>76</sup> However, regeneration in batch mode is not always useful in designing regeneration strategies in packed-bed reactors due to the large differences in specific surface area (i.e., catalyst surface area/solution volume). Additional work in Pd–In/γ-Al<sub>2</sub>O<sub>3</sub> packed-bed reactors showed that significant dissolution of Pd occurred in unbuffered HOCl/OCl<sup>−</sup> solutions.<sup>197</sup> A significant pH drop

in unbuffered solutions results from the oxidation of bound S<sup>2−</sup> to S<sup>6+</sup> on Pd and In sites, as shown in eqs 4 and 5.



Buffering with NaHCO<sub>3</sub> (pH = 8) greatly limited effluent Pd concentrations, but some Pd mobilization still occurred during regeneration.<sup>197</sup> Studies focused on TCE reduction have reported near complete regeneration of S-fouled Pd/γ-Al<sub>2</sub>O<sub>3</sub> catalysts in packed-bed reactors using frequent regeneration with HOCl/OCl<sup>−</sup> solutions; however, catalyst stability was not monitored.<sup>170,175,176</sup> Therefore, it is not clear whether the catalyst was completely stable or if Pd dissolution occurred but catalyst activity remained high due to an excess of Pd. Alternative regeneration strategies have used MnO<sub>4</sub><sup>−</sup> as an oxidant at a pH of 3.0 for S-fouled Pd/γ-Al<sub>2</sub>O<sub>3</sub> catalysts.<sup>198,199</sup> Although regeneration appeared to completely restore catalyst activity, as measured by TCE reduction, the catalyst stability was not monitored and regeneration was only performed in batch mode. Further work is needed to evaluate MnO<sub>4</sub><sup>−</sup> regeneration in packed-bed reactors and detailed characterization of the catalyst structure before and after regeneration.

Other water foulants are less problematic and regeneration can readily regain catalyst activity. It has been shown that NOM fouling was reversible upon an alkaline rinse (NaOH; pH 11),<sup>171</sup> and mineral precipitation could be removed by an acid rinse.<sup>179</sup> However, work has not yet been done on determining the effects of acid and base regeneration on catalyst and/or support stability. Regeneration of catalysts fouled by redox active metals has not been explored, but oxidative regeneration should be a promising starting point.

**2.4. Technology Applications.** The technical and economic feasibility of Pd-based catalytic water treatment has been demonstrated at three groundwater sites contaminated with chlorinated ethenes,<sup>170,191,192</sup> and one contaminated with NO<sub>3</sub><sup>−</sup>.<sup>179</sup> Factors that need to be considered when implementing catalytic groundwater treatment systems include water quality goals, groundwater hydrology, infrastructure, analytical and maintenance support, climate, and hydrogen safety. The system at the Lawrence Livermore National Laboratory (LLNL), California has been in operation since 1999, and was designed to meet the regulatory requirement for in situ treatment of chlorinated solvents (i.e., reactor column was installed below-ground inside a 20-cm well).<sup>191</sup> Groundwater contaminated with chlorinated solvents (TCE, PCE, 1,1-DCE, chloroform) was saturated with hydrogen via a hollow-fiber membrane module (120 mL/min at 3 atm), contacted with two packed-bed catalyst reactors, and returned to the aquifer. The first and the second reactor columns were packed with 30 kg of 3.2-mm and 22 kg of 1.6-mm 1 wt % Pd/γ-Al<sub>2</sub>O<sub>3</sub> catalyst spheres, respectively. The reactors treat 4 L/min at residence times of approximately 5–6 min. Initial removals of TCE, PCE, 1,1-DCE, and chloroform were 93%, 82%, 96%, and 57%, respectively, and have been stable for 10 years utilizing the same catalyst (Walt McNab, LLNL, personal communication). The reactor is operated daily for 6–10 h, followed by flushing with aerobic groundwater, and exposing to air to prevent fouling by anaerobic bacteria.

A similar reactor design was evaluated at the Edwards Air Force Base, California.<sup>170</sup> The groundwater was contaminated with 500–1200  $\mu\text{g/L}$  TCE, was “borderline anoxic” ( $<0.5$  mg/L DO and 3.2 mg/L  $\text{NO}_3^-$ ), contained 760 mg/L  $\text{SO}_4^{2-}$ , and was prone to microbial sulfidogenesis. The packed-bed reactor contained 20 kg of catalyst (6.25-mm alumina beads, eggshell coated with 2 wt % Pd), and was operated continuously for 23 h at 7.6 L/min and a residence time of 2.3 min. Catalyst activity was maintained by daily flushing with dilute  $\text{HOCl/OCl}^-$  (500 mg/L) for 1 h. Hydrogen gas was added by means of a low-pressure frit and a static mixture to achieve 80% of  $\text{H}_2$  saturation (1.7 mg/L at 25 °C and 1 atm). The average effluent TCE concentration was 4.1  $\mu\text{g/L}$ , which was below the maximum contaminant limit of 5  $\mu\text{g/L}$ . During a 23-h treatment cycle slight catalyst deactivation was observed, and was attributed to microbially induced sulfide fouling.

Schüth et al.<sup>192</sup> describe the application of a “fouling-resistant” catalyst with 0.4 wt % Pd on a hydrophobic zeolite Y (Si/Al ratio 200) support<sup>93</sup> at a groundwater site in Germany where groundwater was contaminated with PCE, TCE, and their biological dechlorination products (DCE and vinyl chloride). The packed-bed flow-through reactor consisted of 20 kg of catalyst and was followed by a granular activated carbon (GAC) reactor for final polishing. Hydrogen saturation of the groundwater under atmospheric pressure is achieved by contacting the pumped water with a silicon tube (0.2 cm i.d., 0.4 cm OD, 100 m length, closed at one end) that is pressurized with hydrogen gas produced from a hydrogen generator. The reactor showed sustained removal efficiencies for 2 years, with half-lives of 1.5–3.0 min, in the absence of sulfide fouling. Heavily fouled catalysts could be regenerated to their original state with  $\text{H}_2\text{O}_2$  rinsing.

Davie et al. performed a cost analysis of the Edwards project and indicated that Pd catalysis is competitive with GAC treatment.<sup>170</sup> Catalyst costs are low because lifetimes are long and catalysts can be regenerated on-site. At similar TCE concentrations, treatment costs of Pd-catalysis are comparable to air stripping (not considering costs for treatment of the secondary waste stream in the latter).<sup>170</sup> However, compared to GAC adsorption, the cost advantage of catalytic treatment in general increases with increasing feed concentration, due to the first-order degradation kinetics, and poor adsorption of less chlorinated ethenes (e.g., DCE and vinyl chloride) on GAC. A more detailed cost comparison between GAC and Pd catalytic treatment has been provided by Bayer and Schüth for chlorinated ethenes.<sup>204</sup> The authors compared the major cost factors for GAC adsorption and catalytic hydrodechlorination. All costs extraneous to the treatment process, such as pumping and monitoring, were excluded. In their analysis, the comparative costs are mainly influenced by the Freundlich sorption parameters of GAC and the catalytic dechlorination rates for the contaminants. As a result of sorption nonlinearity, the competitiveness of catalytic dechlorination exceeds GAC treatment for a given compound at relatively high aqueous concentrations. Similarly, catalytic dechlorination is more competitive for compounds that adsorb relatively poorly onto GAC but are dechlorinated rapidly, such as vinyl chloride. The results from Bayer and Schüth<sup>204</sup> are consistent with those from Davie et al.<sup>170</sup> Alternative hydrogen carriers such as formic acid may be considered for safety reasons, as formic acid decomposes to form  $\text{H}_2$  and  $\text{CO}_2$  at the Pd surface.<sup>62,75</sup> However, this would likely increase operational costs. Safety concerns can be addressed by incorporating appropriate engineering design and

safety measures, such as “on demand” electrolytic hydrogen generation and hydrogen sensors linked to interlocks.

Ex situ catalytic nitrate reduction of groundwater was evaluated for a  $\text{NO}_3^-$  concentration of 18 mg/L as N.<sup>179</sup> The optimal system consisted of three packed-bed reactors in series with a liquid flow rate of 7  $\text{m}^3/\text{h}$ . The three reactors were designed to catalytically reduce DO (30 kg of 1.0 wt %Pd/ $\gamma$ -alumina catalyst),  $\text{NO}_3^-$  (200 kg of 1.0 wt %Pd-0.25 wt %Cu/ $\gamma$ -alumina), and  $\text{NO}_2^-$  (150 kg of 1.0 wt %Pd/ $\gamma$ -alumina catalyst) sequentially. The water was saturated with  $\text{H}_2$  (reductant) and  $\text{CO}_2$  (buffer pH) by membrane modules and treated with NaOCl to kill biological growth before entering the reactors. Although the system was able to reduce  $\text{NO}_3^-$  below the MCL (10 mg/L as N), it could not sustainably achieve levels of  $\text{NH}_4^+$  below the World Health Organization limit of 0.5 mg/L.<sup>159</sup> Fouling by biological growth and precipitation of salts on the catalyst both affected performance.

### 3. IDENTIFICATION AND PRIORITIZATION OF FUTURE RESEARCH

Future research should be aimed at (1) improving the basic science of aqueous heterogeneous catalytic transformation processes, (2) identifying and overcoming current barriers to technology implementation and advancing the development of integrated treatment processes, and (3) assessing the economics and environmental implications of using catalytic reduction processes for water treatment and remediation.

**1. Basic Science.** Future experimental work on aqueous Pd-based catalytic treatment needs to be complemented with advanced spectroscopic techniques (e.g., XAFS, ATR-FTIR, STEM, SERS) and atomistic simulations (e.g., DFT) to advance understanding of molecular-scale processes that underpin the macroscopically observed transformation processes and rates. Although there is a rich literature concerning heterogeneous gas-phase catalysis, the understanding of catalysis at the metal–aqueous interface remains in its infancy. Computational methods describing the metal– $\text{H}_2\text{O}$  interface in the presence of ionic adsorbates are needed. Experimental work should also focus on obtaining improved insights into the relationships between contaminant structure and reactivity with Pd-based catalysts in an effort to develop useful predictive models (QSARs, LFERs). Work is also needed to identify how the catalyst structure is related to the observed catalytic performance, because for some contaminants slow reduction rates translate into prohibitively high catalyst costs. Specifically, the *active sites* for contaminant reduction, and mechanisms by which addition of selected bimetals and other additives enhances catalyst reactions with selected classes of contaminants need to be explored. Additionally, more in situ experiments (e.g., ATR-FTIR) need to be conducted that will provide information on important adsorbed intermediates, and thus will aid in the determination of reaction pathways. Further collaborative studies among researchers from various disciplines (e.g., environmental engineers, chemical engineers, and material scientists) are needed to accomplish these goals.

**2. Identifying Barriers to Implementation and Development of Integrated Treatment Processes.** Practical implementation of catalytic reduction processes has been limited due to catalyst fouling. Further efforts are needed at pilot- and demonstration-scales in field settings to identify technology barriers and facilitate the development of practical strategies for overcoming these hurdles. Despite promising findings from field studies conducted to date,<sup>170,191,192</sup> much

more research is needed to demonstrate long-term successful treatment at a variety of field sites and with diverse classes of contaminants.

Work is also needed to couple catalytic reduction processes with other treatment technologies in hybrid approaches. Some hybrid technologies have been studied, such as using adsorbents to remove contaminants from contaminated water, and then treating the concentrated contaminants off-stream following desorption from the adsorbents (e.g., hybrid ion exchange/catalytic reduction of nitrate).<sup>205–207</sup>

**3. Economics and Environmental Implications.** Finally, any pilot and field demonstrations need to incorporate a full analysis of capital and operating costs that can be readily used to assess costs in scaled up processes, enabling engineers and regulators to make more informed decisions on technology selection at individual sites. In addition to cost considerations, it is also imperative that the ultimate environmental sustainability of processes be considered when selecting technologies for site cleanup or water treatment. New tools and approaches in life cycle analysis permit comparison of the environmental footprints of different remediation processes. Therefore, work is needed to compare catalytic reduction processes with other technologies, considering resources and energy inputs into the various processes, as well as waste byproducts and the impacts of processes in terms of various metrics (e.g., global warming potential, ozone depletion potential, eutrophication, etc.). With this type of comparison, windows of application could be defined for catalytic reduction with respect to competing technologies.

## ■ ASSOCIATED CONTENT

### ■ Supporting Information

Reaction pathways for contaminants, reaction rate constants, and reaction conditions for data shown in Figure 2, and calculation of bond strengths for oxyanions shown in Table 2. This material is available free of charge via the Internet at <http://pubs.acs.org>.

## ■ AUTHOR INFORMATION

### Corresponding Author

\*Phone: 217-333-3822; fax: 217-33-6968; e-mail: [werth@illinois.edu](mailto:werth@illinois.edu).

### Notes

The authors declare no competing financial interest.

## ■ ACKNOWLEDGMENTS

Partial support for W.F.S., J.R.S., T.J.S., and C.J.W. was provided by Water CAMPWS, a Science and Technology Center program of the National Science Foundation, under agreement CTS-0120978. Partial support for J.R.S., T.J.S., and C.J.W. was also provided by NSF Chemical, Bioengineering, Environmental, and Transport Systems under agreement CBET 07-30050. Partial support for B.P.C. was provided by Villanova University. Partial support for C.S. was provided by the German Federal Ministry for Education and Research. We thank Ms. Adrienne Donaghue for copy editing the manuscript.

## ■ REFERENCES

- (1) Horold, S.; Vorlop, K. D.; Tacke, T.; Sell, M. Development of catalysts for a selective nitrate and nitrite removal from drinking water. *Catal. Today* **1993**, *17* (1–2), 21–30.
- (2) Pintar, A.; Bercic, G.; Levec, J. Catalytic liquid-phase nitrite reduction: Kinetics and catalyst deactivation. *AIChE J.* **1998**, *44* (10), 2280–2292.

- (3) Shuai, D.; Chaplin, B. P.; Shapley, J. R.; Menendez, N. P.; McCalman, D. C.; Schneider, W. F.; Werth, C. J. Enhancement of oxyanion and diatrizoate reduction kinetics using selected azo dyes on Pd-based catalysts. *Environ. Sci. Technol.* **2010**, *44* (5), 1773–1779.

- (4) Hurley, K. D.; Shapley, J. R. Efficient heterogeneous catalytic reduction of perchlorate in water. *Environ. Sci. Technol.* **2007**, *41* (6), 2044–2049.

- (5) Hurley, K. D.; Zhang, Y. X.; Shapley, J. R. Ligand-enhanced reduction of perchlorate in water with heterogeneous Re-Pd/C catalysts. *J. Am. Chem. Soc.* **2009**, *131* (40), 14172.

- (6) Zhang, Y. X.; Hurley, K. D.; Shapley, J. R. Heterogeneous catalytic reduction of perchlorate in water with Re-Pd/C catalysts derived from an oxorhenium(V) molecular precursor. *Inorg. Chem.* **2011**, *50* (4), 1534–1543.

- (7) Davie, M. G.; Reinhard, M.; Shapley, J. R. Metal-catalyzed reduction of *N*-nitrosodimethylamine with hydrogen in water. *Environ. Sci. Technol.* **2006**, *40* (23), 7329–7335.

- (8) Davie, M. G.; Shih, K.; Pacheco, F. A.; Leckie, J. O.; Reinhard, M. Palladium-indium catalyzed reduction of *N*-nitrosodimethylamine: Indium as a promoter metal. *Environ. Sci. Technol.* **2008**, *42* (8), 3040–3046.

- (9) Schreier, C. G.; Reinhard, M. Catalytic hydrodehalogenation of chlorinated ethylenes using palladium and hydrogen for the treatment of contaminated water. *Chemosphere* **1995**, *31* (6), 3475–3487.

- (10) Lowry, G. V.; Reinhard, M. Hydrodehalogenation of 1- to 3-carbon halogenated organic compounds in water using a palladium catalyst and hydrogen gas. *Environ. Sci. Technol.* **1999**, *33* (11), 1905–1910.

- (11) Muftikian, R.; Fernando, Q.; Korte, N. A method for the rapid dechlorination of low molecular weight chlorinated hydrocarbons in water. *Water Res.* **1995**, *29* (10), 2434–2439.

- (12) Kovenklioglu, S.; Cao, Z.; Shah, D.; Farrauto, R. J.; Balko, E. N. Direct catalytic hydrodechlorination of toxic organics in wastewater. *AIChE J.* **1992**, *38* (7), 1003–1012.

- (13) Schuth, C.; Reinhard, M. Hydrodechlorination and hydrogenation of aromatic compounds over palladium on alumina in hydrogen-saturated water. *App. Catal., B* **1998**, *18* (3–4), 215–221.

- (14) Hoke, J. B.; Gramiccioni, G. A.; Balko, E. N. Catalytic hydrodechlorination of chlorophenols. *App. Catal., B* **1992**, *1* (4), 285–296.

- (15) Vorlop, K.-D.; Prüsse, U. Catalytic removing nitrate from water. In *Environmental Catalysis*; Janssen, F. J. G., van Santen, R. A., Eds.; Imperial College Press: London, 1999; p 369.

- (16) Gauthard, F.; Epron, F.; Barbier, J. Palladium and platinum-based catalysts in the catalytic reduction of nitrate in water: Effect of copper, silver, or gold addition. *J. Catal.* **2003**, *220* (1), 182–191.

- (17) Mikami, I.; Sakamoto, Y.; Yoshinaga, Y.; Okuhara, T. Kinetic and adsorption studies on the hydrogenation of nitrate and nitrite in water using Pd-Cu on active carbon support. *Appl. Catal., B* **2003**, *44* (1), 79–86.

- (18) Mikami, I.; Yoshinaga, Y.; Okuhara, T. Rapid removal of nitrate in water by hydrogenation to ammonia with Zr-modified porous Ni catalysts. *Appl. Catal., B* **2004**, *49* (3), 173–179.

- (19) Soares, O.; Orfao, J. J. M.; Pereira, M. F. R. Activated carbon supported metal catalysts for nitrate and nitrite reduction in water. *Catal. Lett.* **2008**, *126* (3–4), 253–260.

- (20) Marchesini, F. A.; Irusta, S.; Querini, C.; Miro, E. Nitrate hydrogenation over Pt<sub>2</sub>In/Al<sub>2</sub>O<sub>3</sub> and Pt<sub>2</sub>In/SiO<sub>2</sub>. Effect of aqueous media and catalyst surface properties upon the catalytic activity. *Catal. Commun.* **2008**, *9* (6), 1021–1026.

- (21) Rylander, P. N. *Hydrogenation Methods*; Academic Press: New York, 1985.

- (22) Calvo, L.; Gilarranz, M. A.; Casas, J. A.; Mohedano, A. F.; Rodriguez, J. J. Denitrification of water with activated carbon-supported metallic catalysts. *Ind. Eng. Chem. Res.* **2010**, *49* (12), 5603–5609.

- (23) Weidlich, T.; Krejcova, A.; Prokes, L. Study of dehalogenation of halogenoanilines using Raney Al-Ni alloy in aqueous medium at room temperature. *Mon. Chem.* **2010**, *141* (9), 1015–1020.

- (24) Brylev, O.; Sarrazin, M.; Belanger, D.; Roue, L. Rhodium deposits on pyrolytic graphite substrate: Physico-chemical properties and electrocatalytic activity towards nitrate reduction in neutral medium. *Appl. Catal., B* **2006**, *64* (3–4), 243–253.
- (25) Witonska, I.; Karski, S.; Goluchowska, J. Kinetic studies on the hydrogenation of nitrate in water using Rh/Al<sub>2</sub>O<sub>3</sub> and Rh-Cu/Al<sub>2</sub>O<sub>3</sub> catalysts. *Kinet. Catal.* **2007**, *48* (6), 823–828.
- (26) Soares, O.; Orfao, J. J. M.; Pereira, M. F. R. Bimetallic catalysts supported on activated carbon for the nitrate reduction in water: Optimization of catalysts composition. *Appl. Catal., B* **2009**, *91* (1–2), 441–448.
- (27) Frierdich, A. J.; Shapley, J. R.; Strathmann, T. J. Rapid reduction of *N*-nitrosamine disinfection byproducts in water with hydrogen and porous nickel catalysts. *Environ. Sci. Technol.* **2008**, *42* (1), 262–269.
- (28) Frierdich, A. J.; Joseph, C. E.; Strathmann, T. J. Catalytic reduction of *N*-nitrosodimethylamine with nanophase nickel-boron. *Appl. Catal., B* **2009**, *90* (1–2), 175–183.
- (29) Kasprzak, K. S.; Sunderman, F. W.; Salnikow, K. Nickel carcinogenesis. *Mutat. Res., Fundam. Mol. Mech. Mutagen.* **2003**, *533* (1–2), 67–97.
- (30) Dunnick, J. K.; Elwell, M. R.; Radovsky, A. E.; Benson, J. M.; Hahn, F. F.; Nikula, K. J.; Barr, E. B.; Hobbs, C. H. Comparative carcinogenic effects of nickel subsulfide, nickel-oxide, or nickel sulfate hexahydrate chronic exposures in the lung. *Cancer Res.* **1995**, *55* (22), 5251–5256.
- (31) Kelley, R. D.; Candela, G. A.; Madey, T. E.; Newbury, D. E.; Schehl, R. R. Surface and bulk analysis of a deactivated Raney-nickel methanation catalyst. *J. Catal.* **1983**, *80* (2), 235–248.
- (32) Petro, J.; Bota, A.; Laszlo, K.; Beyer, H.; Kalman, E.; Dodony, I. A new alumina-supported, not pyrophoric Raney-type Ni-catalyst. *Appl. Catal., A* **2000**, *190* (1–2), 73–86.
- (33) Wang, D. M.; Shah, S. I.; Chen, J. G.; Huang, C. P. Catalytic reduction of perchlorate by H<sub>2</sub> gas in dilute aqueous solutions. *Sep. Purif. Technol.* **2008**, *60* (1), 14–21.
- (34) Mahmudov, R.; Shu, Y. Y.; Rykov, S.; Chen, J. G.; Huang, C. P. The reduction of perchlorate by hydrogenation catalysts. *Appl. Catal., B* **2008**, *81* (1–2), 78–87.
- (35) Wang, D. M.; Huang, C. P.; Chen, J. G.; Lin, H. Y.; Shah, S. I. Reduction of perchlorate in dilute aqueous solutions over mono-metallic nano-catalysts: Exemplified by tin. *Sep. Purif. Technol.* **2007**, *58* (1), 129–137.
- (36) Wang, D. M.; Huang, C. P. Electrodiallytically assisted catalytic reduction (EDACR) of perchlorate in dilute aqueous solutions. *Sep. Purif. Technol.* **2008**, *59* (3), 333–341.
- (37) Alowitz, M. J.; Scherer, M. M. Kinetics of nitrate, nitrite, and Cr(VI) reduction by iron metal. *Environ. Sci. Technol.* **2002**, *36* (3), 299–306.
- (38) Jiang, Z. M.; Lv, L.; Zhang, W. M.; Du, Q. O.; Pan, B. C.; Yang, L.; Zhang, Q. X. Nitrate reduction using nanosized zero-valent iron supported by polystyrene resins: Role of surface functional groups. *Water Res.* **2011**, *45* (6), 2191–2198.
- (39) Matatov-Meytal, U.; Sheintuch, M. Activated carbon cloth-supported Pd-Cu catalyst: Application for continuous water denitrification. *Catal. Today* **2005**, *102*, 121–127.
- (40) Nakamura, K.; Yoshida, Y.; Mikami, I.; Okuhara, T. Selective hydrogenation of nitrate in water over Cu-Pd/mordenite. *Appl. Catal., B* **2006**, *65* (1–2), 31–36.
- (41) Xie, Y. B.; Cao, H. B.; Li, Y. P.; Zhang, Y.; Crittenden, J. C. Highly selective PdCu/amorphous silica-alumina (ASA) catalysts for groundwater denitrification. *Environ. Sci. Technol.* **2011**, *45* (9), 4066–4072.
- (42) Lien, H. L.; Zhang, W. X. Transformation of chlorinated methanes by nanoscale iron particles. *J. Environ. Eng. Div. (Am Soc. Civ. Eng.)* **1999**, *125* (11), 1042–1047.
- (43) Nurmi, J. T.; Tratnyek, P. G.; Sarathy, V.; Baer, D. R.; Amonette, J. E.; Pecher, K.; Wang, C. M.; Linehan, J. C.; Matson, D. W.; Penn, R. L.; Driessen, M. D. Characterization and properties of metallic iron nanoparticles: Spectroscopy, electrochemistry, and kinetics. *Environ. Sci. Technol.* **2005**, *39* (5), 1221–1230.
- (44) Farrell, J.; Kason, M.; Melitas, N.; Li, T. Investigation of the long-term performance of zero-valent iron for reductive dechlorination of trichloroethylene. *Environ. Sci. Technol.* **2000**, *34* (3), S14–S21.
- (45) Sarathy, V.; Tratnyek, P. G.; Nurmi, J. T.; Baer, D. R.; Amonette, J. E.; Chun, C. L.; Penn, R. L.; Reardon, E. J. Aging of iron nanoparticles in aqueous solution: Effects on structure and reactivity. *J. Phys. Chem. C* **2008**, *112* (7), 2286–2293.
- (46) Crittenden, J. C.; Trussell, R. R.; Hand, D. W.; Howe, K. J.; Tchobanoglous, G. *Water Treatment: Principles and Design*; John Wiley and Sons: Hoboken, NJ, 2005.
- (47) Krasner, S. W.; McGuire, M. J.; Jacangelo, J. G.; Patania, N. L.; Reagan, K. M.; Aieta, E. M. The occurrence of disinfection by-products in United-States drinking-water. *J. Am. Water Works Assoc.* **1989**, *81* (8), 41–53.
- (48) Richardson, S. D.; Plewa, M. J.; Wagner, E. D.; Schoeny, R.; DeMarini, D. M. Occurrence, genotoxicity, and carcinogenicity of regulated and emerging disinfection by-products in drinking water: A review and roadmap for research. *Mutat. Res., Rev. Mutat. Res.* **2007**, *636* (1–3), 178–242.
- (49) Mitch, W. A.; Sharp, J. O.; Trussell, R. R.; Valentine, R. L.; Alvarez-Cohen, L.; Sedlak, D. L. *N*-nitrosodimethylamine (NDMA) as a drinking water contaminant: A review. *Environ. Eng. Sci.* **2003**, *20* (5), 389–404.
- (50) Andrzejewski, P.; Kasprzyk-Hordern, B.; Nawrocki, J. *N*-nitrosodimethylamine (NDMA) formation during ozonation of dimethylamine-containing waters. *Water Res.* **2008**, *42* (4–5), 863–870.
- (51) Andrzejewski, P.; Nawrocki, J. *N*-nitrosodimethylamine formation during treatment with strong oxidants of dimethylamine containing water. *Water Sci. Technol.* **2007**, *56* (12), 125–131.
- (52) Nerenberg, R.; Rittmann, B. E.; Najm, I. Perchlorate reduction in a hydrogen-based membrane-biofilm reactor. *J. Am. Water Works Assoc.* **2002**, *94* (11), 103–114.
- (53) Ziv-El, M. C.; Rittmann, B. E. Systematic evaluation of nitrate and perchlorate bioreduction kinetics in groundwater using a hydrogen-based membrane biofilm reactor. *Water Res.* **2009**, *43* (1), 173–181.
- (54) Rittmann, B. E. Environmental biotechnology in water and wastewater treatment. *J. Environ. Eng. (Am. Soc. Civ. Eng.)* **2010**, *136* (4), 348–353.
- (55) Hildebrand, H.; Mackenzie, K.; Kopinke, F. D. Highly active Pd-on-magnetite nanocatalysts for aqueous phase hydrodechlorination reactions. *Environ. Sci. Technol.* **2009**, *43* (9), 3254–3259.
- (56) Hildebrand, H.; Mackenzie, K.; Kopinke, F. D. Novel nano-catalysts for wastewater treatment. *Glob. Nest. J.* **2008**, *10* (1), 47–53.
- (57) Nutt, M. O.; Hughes, J. B.; Wong, M. S. Designing Pd-on-Au bimetallic nanoparticle catalysts for trichloroethene hydrodechlorination. *Environ. Sci. Technol.* **2005**, *39* (5), 1346–1353.
- (58) Nutt, M. O.; Heck, K. N.; Alvarez, P. J. J.; Wong, M. S. Improved Pd-on-Au bimetallic nanoparticle catalysts for aqueous-phase trichloroethene hydrodechlorination. *Appl. Catal., B* **2006**, *69* (1–2), 115–125.
- (59) Wong, M. S.; Alvarez, P. J. J.; Fang, Y. I.; Akcin, N.; Nutt, M. O.; Miller, J. T.; Heck, K. N. Cleaner water using bimetallic nanoparticle catalysts. *J. Chem. Technol. Biotechnol.* **2009**, *84* (2), 158–166.
- (60) Fang, Y. L.; Heck, K. N.; Alvarez, P. J. J.; Wong, M. S. Kinetics analysis of palladium/gold nanoparticles as colloidal hydrodechlorination catalysts. *ACS Catal.* **2011**, *1* (2), 128–138.
- (61) Pintar, A.; Batista, J.; Levec, J.; Kajiuchi, T. Kinetics of the catalytic liquid-phase hydrogenation of aqueous nitrate solutions. *Appl. Catal., B* **1996**, *11* (1), 81–98.
- (62) Prusse, U.; Vorlop, K.-D. Supported bimetallic palladium catalysts for water-phase nitrate reduction. *J. Mol. Catal. A: Chem.* **2001**, *173* (1–2), 313–328.
- (63) Cwiertny, D. M.; Bransfield, S. J.; Livi, K. J. T.; Fairbrother, D. H.; Roberts, A. L. Exploring the influence of granular iron additives on 1,1,1-trichloroethane reduction. *Environ. Sci. Technol.* **2006**, *40* (21), 6837–6843.

- (64) He, F.; Zhao, D. Y. Hydrodechlorination of trichloroethene using stabilized Fe-Pd nanoparticles: Reaction mechanism and effects of stabilizers, catalysts and reaction conditions. *Appl. Catal., B* **2008**, *84* (3–4), 533–540.
- (65) Choi, J. H.; Shin, W. S.; Choi, S. J.; Kim, Y. H. Reductive denitrification using zero-valent iron and bimetallic iron. *Environ. Technol.* **2009**, *30* (9), 939–946.
- (66) Dittmeyer, R.; Hollein, V.; Daub, K. Membrane reactors for hydrogenation and dehydrogenation processes based on supported palladium. *J. Mol. Catal. A: Chem.* **2001**, *173* (1–2), 135–184.
- (67) Urbano, F. J.; Marinas, J. M. Hydrogenolysis of organohalogen compounds over palladium supported catalysts. *J. Mol. Catal. A: Chem.* **2001**, *173* (1–2), 329–345.
- (68) Pirkanniemi, K.; Sillanpaa, M. Heterogeneous water phase catalysis as an environmental application: A review. *Chemosphere* **2002**, *48* (10), 1047–1060.
- (69) Amorim, C.; Yuan, G.; Patterson, P. M.; Keane, M. A. Catalytic hydrodechlorination over Pd supported on amorphous and structured carbon. *J. Catal.* **2005**, *234* (2), 268–281.
- (70) Keane, M. A. A review of catalytic approaches to waste minimization: Case study - liquid-phase catalytic treatment of chlorophenols. *J. Chem. Technol. Biotechnol.* **2005**, *80* (11), 1211–1222.
- (71) Barrabes, N.; Sa, J. Catalytic nitrate removal from water, past, present and future perspectives. *Appl. Catal., B* **2011**, *104* (1–2), 1–5.
- (72) Keane, M. A. Supported transition metal catalysts for hydrodechlorination reactions. *ChemCatChem* **2011**, *3* (5), 800–821.
- (73) Chen, H.; Xu, Z. Y.; Wan, H. Q.; Zheng, J. Z.; Yin, D. Q.; Zheng, S. R. Aqueous bromate reduction by catalytic hydrogenation over Pd/Al<sub>2</sub>O<sub>3</sub> catalysts. *Appl. Catal., B* **2010**, *96* (3–4), 307–313.
- (74) Strukul, G.; Gavagnin, R.; Pinna, F.; Modafferri, E.; Perathoner, S.; Centi, G.; Marella, M.; Tomaselli, M. Use of palladium based catalysts in the hydrogenation of nitrates in drinking water: From powders to membranes. *Catal. Today* **2000**, *55* (1–2), 139–149.
- (75) Prusse, U.; Hahnlein, M.; Daum, J.; Vorlop, K.-D. Improving the catalytic nitrate reduction. *Catal. Today* **2000**, *55* (1–2), 79–90.
- (76) Chaplin, B. P.; Shapley, J. R.; Werth, C. J. Regeneration of sulfur-fouled bimetallic Pd-based catalysts. *Environ. Sci. Technol.* **2007**, *41* (15), 5491–5497.
- (77) Conrad, H.; Ertl, G.; Latta, E. E. Adsorption of hydrogen on palladium single crystal surfaces. *Surf. Sci.* **1974**, *41* (2), 435–446.
- (78) Uemiyu, S.; Matsuda, T.; Kikuchi, E. Hydrogen permeable palladium silver alloy membrane supported on porous ceramics. *J. Membr. Sci.* **1991**, *56* (3), 315–325.
- (79) Uemiyu, S.; Sato, N.; Ando, H.; Kude, Y.; Matsuda, T.; Kikuchi, E. Separation of hydrogen through palladium thin-film supported on a porous-glass tube. *J. Membr. Sci.* **1991**, *56* (3), 303–313.
- (80) Khanuja, M.; Mehta, B. R.; Agar, P.; Kulriya, P. K.; Avasthi, D. K., Hydrogen induced lattice expansion and crystallinity degradation in palladium nanoparticles: Effect of hydrogen concentration, pressure, and temperature. *J. Appl. Phys.* **2009**, *106* (9).
- (81) Crespo, E. A.; Claramonte, S.; Ruda, M.; de Debiaggi, S. R. Thermodynamics of hydrogen in Pd nanoparticles. *Int. J. Hydrogen Energy* **2010**, *35* (11), 6037–6041.
- (82) Teschner, D.; Borsodi, J.; Kis, Z.; Szentmiklosi, L.; Revay, Z.; Knop-Gericke, A.; Schlögl, R.; Torres, D.; Sautet, P. Role of hydrogen species in palladium-catalyzed alkyne hydrogenation. *J. Phys. Chem. C* **2010**, *114* (5), 2293–2299.
- (83) Tierney, H. L.; Baber, A. E.; Kitchin, J. R.; Sykes, E. C. H. Hydrogen dissociation and spillover on individual isolated palladium atoms. *Phys. Rev. Lett.* **2009**, *103* (24).
- (84) Choe, J. K.; Shapley, J. R.; Strathmann, T. J.; Werth, C. J. Influence of rhenium speciation on the stability and activity of Re/Pd bimetal catalysts used for perchlorate reduction. *Environ. Sci. Technol.* **2010**, *44* (12), 4716–4721.
- (85) Yoshinaga, Y.; Akita, T.; Mikami, I.; Okuhara, T. Hydrogenation of nitrate in water to nitrogen over Pd-Cu supported on active carbon. *J. Catal.* **2002**, *207* (1), 37–45.
- (86) Chaplin, B. P.; Roundy, E.; Guy, K. A.; Shapley, J. R.; Werth, C. J. Effects of natural water ions and humic acid on catalytic nitrate reduction kinetics using an alumina supported Pd-Cu catalyst. *Environ. Sci. Technol.* **2006**, *40* (9), 3075–3081.
- (87) Zhang, F. X.; Miao, S.; Yang, Y. L.; Zhang, X.; Chen, J. X.; Guan, N. J. Size-dependent hydrogenation selectivity of nitrate on Pd-Cu/TiO<sub>2</sub> catalysts. *J. Phys. Chem. C* **2008**, *112* (20), 7665–7671.
- (88) Daub, K.; Emig, G.; Chollier, M. J.; Callant, M.; Dittmeyer, R. Studies on the use of catalytic membranes for reduction of nitrate in drinking water. *Chem. Eng. Sci.* **1999**, *54* (10), 1577–1582.
- (89) Gavagnin, R.; Biasetto, L.; Pinna, F.; Strukul, G. Nitrate removal in drinking waters: The effect of tin oxides in the catalytic hydrogenation of nitrate by Pd/SnO<sub>2</sub> catalysts. *Appl. Catal., B* **2002**, *38* (2), 91–99.
- (90) Neyertz, C.; Marchesini, F. A.; Boix, A.; Miro, E.; Querini, C. A. Catalytic reduction of nitrate in water: Promoted palladium catalysts supported in resin. *Appl. Catal., A* **2010**, *372* (1), 40–47.
- (91) Dodouche, I.; Barbosa, D. P.; Rangel, M. D.; Epron, F. Palladium-tin catalysts on conducting polymers for nitrate removal. *Appl. Catal., B* **2009**, *93* (1–2), 50–55.
- (92) Chinthaginjala, J. K.; Bitter, J. H.; Lefferts, L. Thin layer of carbon-nano-fibers (CNFS) as catalyst support for fast mass transfer in hydrogenation of nitrite. *Appl. Catal., A* **2010**, *383* (1–2), 24–32.
- (93) Schuth, C.; Disser, S.; Schuth, F.; Reinhard, M. Tailoring catalysts for hydrodechlorinating chlorinated hydrocarbon contaminants in groundwater. *Appl. Catal., B* **2000**, *28* (3–4), 147–152.
- (94) Gregg, S. J.; Sing, K. W. W. *Adsorption, Surface Area, and Porosity*; Academic Press, 1982.
- (95) Bradshaw, A. M.; Hoffmann, F. M. The chemisorption of carbon monoxide on palladium single crystal surfaces: Ir spectroscopic evidence for localised site adsorption. *Surf. Sci.* **1978**, *72* (3), 513–553.
- (96) Crozier, P. A. Nanocharacterization of Heterogeneous Catalysts by Ex-situ and In-situ stem. In *Scanning Transmission Electron Microscopy, Imaging and Analysis*; Pennycook, S. J., Nellist, P. D., Eds.; Springer, 2011.
- (97) Liu, J. Advanced electron microscopy characterization of nanostructured heterogeneous catalysts. *Microsc. Microanal.* **2004**, *10*, 55–76.
- (98) Longergan, W. W.; Vlachos, D. G.; Chen, J. G. G. Correlating extent of Pt-Ni bond formation with low-temperature hydrogenation of benzene and 1,3 butadiene over supported Pt/Ni bimetallic catalysts. *J. Catal.* **2010**, *271* (2), 239–250.
- (99) Alexeev, O. S.; Krishnamoorthy, S.; Ziebarth, M. S.; Yaluri, G.; Roberie, T. G.; Amiridis, M. D. Characterization of Pd-based FCCO/NO<sub>x</sub> control additives by in situ FTIR and extended X-ray adsorption fine spectroscopies. *Catal. Today* **2007**, *127* (1–4), 176–188.
- (100) Consul, J. M. D.; Baibich, I. M.; Alves, M. C. M. XANES investigation of the enhanced chemical stability of Pd in supported Pd-Mo catalysts. *Catal. Commun.* **2011**, *12* (14), 1357–1360.
- (101) Wachs, I. E. *Characterization of Catalytic Materials*; Materials Characterization Series, Brundle, C. R., Evans, J. C. A., Eds.; Momentum Press, 2009.
- (102) Niemantsverdriet, J. W. *Spectroscopy in Catalysis: An Introduction*, 3rd ed.; Wiley: New York, 2007.
- (103) Somorjai, G. A.; Yimin, L. *Introduction to Surface Chemistry and Catalysis*; John Wiley & Sons: New York, 2010.
- (104) Siantar, D. P.; Schreier, C. G.; Chou, C. S.; Reinhard, M. Treatment of 1,2-dibromo-3-chloropropane and nitrate-contaminated water with zero-valent iron or hydrogen/palladium catalysts. *Water Res.* **1996**, *30* (10), 2315–2322.
- (105) Maia, M. P.; Rodrigues, M. A.; Passos, F. B. Nitrate catalytic reduction in water using niobia supported palladium-copper catalysts. *Catal. Today* **2007**, *123* (1–4), 171–176.
- (106) Constantinou, C. L.; Costa, C. N.; Efstathiou, A. M. The remarkable effect of oxygen on the N<sub>2</sub> selectivity of water catalytic denitrification by hydrogen. *Environ. Sci. Technol.* **2007**, *41* (3), 950–956.
- (107) Chinthaginjala, J. K.; Lefferts, L. Support effect on selectivity of nitrite reduction in water. *Appl. Catal., B* **2010**, *101* (1–2), 144–149.

- (108) Soares, O.; Orfao, J. J. M.; Pereira, M. F. R. Nitrate reduction catalyzed by Pd-Cu and Pt-Cu supported on different carbon materials. *Catal. Lett.* **2010**, *139* (3–4), 97–104.
- (109) Soares, O.; Orfao, J. J. M.; Pereira, M. F. R. Nitrate reduction in water catalysed by Pd-Cu on different supports. *Desalination* **2011**, *279* (1–3), 367–374.
- (110) Ealet, B.; Gillet, E. Palladium alumina interface - Influence of the oxide stoichiometry studied by EELS and XPS. *Surf. Sci.* **1993**, *281* (1–2), 91–101.
- (111) Henry, C. R. Surface studies of supported model catalysts. *Surf. Sci. Rep.* **1998**, *31* (7–8), 235–325.
- (112) Baumer, M.; Freund, H.-J. Metal deposits on well-ordered oxide films. *Prog. Surf. Sci.* **1999**, *61* (127).
- (113) Xiao, L.; Schneider, W. F. Surface termination effects on metal atom adsorption on [alpha]-alumina. *Surf. Sci.* **2008**, *602*.
- (114) Xiao, L.; Schneider, W. F. Influence of [alpha]-alumina supports on oxygen binding to Pd, Ag, Pt, and Au. *Chem. Phys. Lett.* **2010**, *484* (231).
- (115) Soares, O.; Orfao, J. J. M.; Pereira, M. F. R. Nitrate reduction with hydrogen in the presence of physical mixtures with mono and bimetallic catalysts and ions in solution. *Appl. Catal., B* **2011**, *102* (3–4), 424–432.
- (116) Karpinski, Z.; Early, K.; dltri, J. L. Catalytic hydrodechlorination of 1,1-dichlorotetrafluoroethane by Pd/Al<sub>2</sub>O<sub>3</sub>. *J. Catal.* **1996**, *164* (2), 378–386.
- (117) Aramendia, M. A.; Borau, V.; Garcia, I. M.; Jimenez, C.; Lafont, F.; Marinas, A.; Marinas, J. M.; Urbano, F. J. Influence of the reaction conditions and catalytic properties on the liquid-phase hydrodechlorination of chlorobenzene over palladium-supported catalysts: Activity and deactivation. *J. Catal.* **1999**, *187* (2), 392–399.
- (118) Aramendia, M. A.; Borau, V.; Garcia, I. M.; Jimenez, C.; Marinas, J. M.; Urbano, F. J. Influence of the reaction conditions and catalytic properties on the liquid-phase hydrodebromination of bromobenzene over palladium supported catalysts: Activity and deactivation. *Appl. Catal., B* **1999**, *20* (2), 101–110.
- (119) Shuai, D.; Kwon-Choe, J.; Shapley, J. R.; Werth, C. J. Enhanced activity and selectivity of carbon nanofiber supported Pd-based catalysts for nitrite reduction. *Environ. Sci. Technol.* **2012**, *46*, No. 10.1021/es203200d.
- (120) Batista, J.; Pintar, A.; Gomilsek, J. P.; Kodre, A.; Bornette, F. On the structural characteristics of [gamma]-alumina-supported Pd-Cu bimetallic catalysts. *Appl. Catal., A* **2001**, *217* (1–2), 55–68.
- (121) Guy, K. A.; Xu, H. P.; Yang, J. C.; Werth, C. J.; Shapley, J. R. Catalytic nitrate and nitrite reduction with Pd-Cu/PVP colloids in water: Composition, structure, and reactivity correlations. *J. Phys. Chem. C* **2009**, *113* (19), 8177–8185.
- (122) Matatov-Meytal, U.; Sheintuch, M. The relation between surface composition of Pd-Cu/ACC catalysts prepared by selective deposition and their denitrification behavior. *Catal. Commun.* **2009**, *10* (8), 1137–1141.
- (123) Soares, O.; Orfao, J. J. M.; Ruiz-Martinez, J.; Silvestre-Albero, J.; Sepulveda-Escribano, A.; Pereira, M. F. R. Pd-Cu/AC and Pt-Cu/AC catalysts for nitrate reduction with hydrogen influence of calcination and reduction temperatures. *Chem. Eng. J.* **2010**, *165* (1), 78–88.
- (124) Chen, N.; Rioux, R. M.; Ribeiro, F. H. Investigation of reaction steps for the hydrodechlorination of chlorine-containing organic compounds on Pd catalysts. *J. Catal.* **2002**, *211* (1), 192–197.
- (125) Chen, N.; Rioux, R. M.; Barbosa, L.; Ribeiro, F. H. Kinetic and theoretical study of the hydrodechlorination of CH<sub>(4-x)</sub>Cl<sub>(x)</sub> (x = 1–4) compounds on palladium. *Langmuir* **2010**, *26* (21), 16615–16624.
- (126) Omar, S.; Palomar, J.; Gomez-Sainero, L. M.; Alvarez-Montero, M. A.; Martin-Martinez, M.; Rodriguez, J. J. Density functional theory analysis of dichloromethane and hydrogen interaction with Pd clusters: First step to simulate catalytic hydrodechlorination. *J. Phys. Chem. C* **2011**, *115* (29), 14180–14192.
- (127) Andersin, J.; Honkala, K. First principles investigations of Pd-on-Au nanostructures for trichloroethene catalytic removal from groundwater. *Phys. Chem. Chem. Phys.* **2011**, *13* (4), 1386–1394.
- (128) Thompson, C. D.; Rioux, R. M.; Chen, N.; Ribeiro, F. H. Turnover rate, reaction order, and elementary steps for the hydrodechlorination of chlorofluorocarbon compounds on palladium catalysts. *J. Phys. Chem. B* **2000**, *104* (14), 3067–3077.
- (129) Kopinke, F.-D.; Mackenzie, K.; Kohler, R. Catalytic hydrodechlorination of groundwater contaminants in water and in the gas phase using Pd/[gamma]-Al<sub>2</sub>O<sub>3</sub>. *Appl. Catal., B* **2003**, *44* (1), 15–24.
- (130) Kovalchuk, V. I.; d'Itri, J. L. Catalytic chemistry of chloro- and chlorofluorocarbon dehalogenation: From macroscopic observations to molecular level understanding. *Appl. Catal., A* **2004**, *271* (1–2), 13–25.
- (131) Sriwatanapongse, W.; Reinhard, M.; Klug, C. A. Reductive hydrodechlorination of trichloroethylene by palladium-on-alumina catalyst: C-13 solid-state NMR study of surface reaction precursors. *Langmuir* **2006**, *22* (9), 4158–4164.
- (132) Heck, K. N.; Janesko, B. G.; Scuseria, G. E.; Halas, N. J.; Wong, M. S. Observing metal-catalyzed chemical reactions in situ using surface-enhanced raman spectroscopy on Pd-Au nanoshells. *J. Am. Chem. Soc.* **2008**, *130* (49), 16592–16600.
- (133) Mackenzie, K.; Frenzel, H.; Kopinke, F. D. Hydrodehalogenation of halogenated hydrocarbons in water with Pd catalysts: Reaction rates and surface competition. *Appl. Catal., B* **2006**, *63* (3–4), 161–167.
- (134) Zhou, G.; Chan, C.; Gellman, A. J. Dechlorination of fluorinated 1,1-dichloroethanes on Pd(111). *J. Phys. Chem. B* **1999**, *103* (7), 1134–1143.
- (135) Rioux, R. M.; Thompson, C. D.; Chen, N.; Ribeiro, F. H. Hydrodechlorination of chlorofluorocarbons CF<sub>3</sub>-CFCl<sub>2</sub> and CF<sub>3</sub>-CCl<sub>3</sub> over Pd/carbon and Pd black catalysts. *Catal. Today* **2000**, *62* (2–3), 269–278.
- (136) Campbell, J. S.; Kemball, C., Catalytic fission of carbon-halogen bond. 2. Reactions of tertiary butyl chloride with hydrogen and deuterium on evaporated platinum and palladium films. *T. Faraday Soc.* **1963**, *59* (491), 2583.
- (137) Gomez-Sainero, L. M.; Seoane, X. L.; Fierro, J. L. G.; Arcoya, A. Liquid-phase hydrodechlorination of CCl<sub>4</sub> to CHCl<sub>3</sub> on Pd/carbon catalysts: Nature and role of Pd active species. *J. Catal.* **2002**, *209* (2), 279–288.
- (138) Barbosa, L.; Loffreda, D.; Sautet, P. Chemisorption of trichloroethene on the PdCu alloy (110) surface: A periodical density functional study. *Langmuir* **2002**, *18* (7), 2625–2635.
- (139) Barbosa, L. A. M. M.; Sautet, P. Trichloroethene dechlorination reactions on the PdCu(110) alloy surface: A periodical density functional theory study of the mechanism. *J. Catal.* **2002**, *207* (1), 127–138.
- (140) Aramendia, M. A.; Borau, V.; Garcia, I. M.; Jimenez, C.; Marinas, A.; Marinas, J. M.; Urbano, F. J. Liquid-phase hydrodehalogenation of substituted chlorobenzenes over palladium supported catalysts. *Appl. Catal., B* **2003**, *43* (1), 71–79.
- (141) Liu, Y.; Yang, F.; Yue, P. L.; Chen, G. Catalytic dechlorination of chlorophenols in water by palladium/iron. *Water Res.* **2001**, *35* (8), 1887–1890.
- (142) Engelmann, M. D.; Hutcheson, R.; Henschied, K.; Neal, R.; Cheng, I. F. Simultaneous determination of total polychlorinated biphenyl and dichlorodiphenyltrichloroethane (DDT) by dechlorination with Fe/Pd and Mg/Pd bimetallic articles and flame ionization detection gas chromatography. *Microchem. J.* **2003**, *74* (1), 19–25.
- (143) da Silva, J. W.; Bruns, R. E.; Cobo, A. J. G. Study of the reaction conditions for the hydrodechlorination of pentachlorophenol on palladium catalysts. *Chem. Eng. J.* **2007**, *131*, 59–64.
- (144) Molina, C. B.; Calvo, L.; Gilaranz, M. A.; Casas, J. A.; Rodriguez, J. J. Pd-Al pillared clays as catalysts for the hydrodechlorination of 4-chlorophenol in aqueous phase. *J. Hazard. Mater.* **2009**, *172* (1), 214–223.
- (145) Ghauch, A.; Tuqan, A. Reductive destruction and decontamination of aqueous solutions of chlorinated antimicrobial agent using bimetallic systems. *J. Hazard. Mater.* **2009**, *164* (2–3), 665–674.

- (146) Patel, U. D.; Suresh, S. Dechlorination of chlorophenols using magnesium-palladium bimetallic system. *J. Hazard. Mater.* **2007**, *147* (1–2), 431–438.
- (147) Yuan, G.; Keane, M. A. Catalyst deactivation during the liquid phase hydrodechlorination of 2,4-dichlorophenol over supported Pd: Influence of the support. *Catal. Today* **2003**, *88* (1–2), 27–36.
- (148) Yuan, G.; Keane, M. A. Liquid phase hydrodechlorination of chlorophenols over Pd/C and Pd/Al<sub>2</sub>O<sub>3</sub>: A consideration of HCl/catalyst interactions and solution pH effects. *Appl. Catal., B* **2004**, *52* (4), 301–314.
- (149) Tian, N.; Zhou, Z. Y.; Sun, S. G. Platinum metal catalysts of high-index surfaces: From single-crystal planes to electrochemically shape-controlled nanoparticles. *J. Phys. Chem. C* **2008**, *112* (50), 19801–19817.
- (150) Roudgar, A.; Gross, A. Local reactivity of metal overlayers: Density functional theory calculations of Pd on Au. *Phys. Rev. B* **2003**, *67* (3), 4.
- (151) Roudgar, A.; Gross, A. Local reactivity of supported metal clusters: Pd-N on Au(111). *Surf. Sci.* **2004**, *559* (2–3), L180–L186.
- (152) Gross, A. Reactivity of bimetallic systems studied from first principles. *Top. Catal.* **2006**, *37* (1), 29–39.
- (153) Gross, A. Tailoring the reactivity of bimetallic overlayer and surface alloy systems. *J. Phys.: Condens. Matter* **2009**, *21* (8), 7.
- (154) Ebbesen, S. D.; Mojet, B. L.; Lefferts, L. In situ ATR-IR study of nitrite hydrogenation over Pd/Al<sub>2</sub>O<sub>3</sub>. *J. Catal.* **2008**, *256*, 15–23.
- (155) Ebbesen, S. D.; Mojet, B. L.; Lefferts, L. In situ attenuated total reflection infrared (ATR-IR) study of the adsorption of NO<sub>2</sub><sup>−</sup>, NH<sub>2</sub>OH, and NH<sub>4</sub><sup>+</sup> on Pd/Al<sub>2</sub>O<sub>3</sub> and Pt/Al<sub>2</sub>O<sub>3</sub>. *Langmuir* **2008**, *24* (3), 869–879.
- (156) Berndt, H.; Monnich, I.; Lucke, B.; Menzel, M. Tin promoted palladium catalysts for nitrate removal from drinking water. *Appl. Catal., B* **2001**, *30* (1–2), 111–122.
- (157) Lemaigen, L.; Tong, C.; Begon, V.; Burch, R.; Chadwick, D. Catalytic denitrification of water with palladium-based catalysts supported on activated carbons. *Catal. Today* **2002**, *75* (1–4), 43–48.
- (158) AbuOmar, M. M.; Appelman, E. H.; Espenson, J. H. Oxygen-transfer reactions of methylrhenium oxides. *Inorg. Chem.* **1996**, *35* (26), 7751–7757.
- (159) WHO. *Guidelines for Drinking Water Quality. Addendum to Volume 2, 2nd ed., Health Criteria and Other Supporting Information (WHO/EOS/98.1)*; World Health Organization: Geneva, 1998.
- (160) Rosca, V.; Duca, M.; de Groot, M. T.; Koper, M. T. M. Nitrogen cycle electrocatalysis. *Chem. Rev.* **2009**, *109* (6), 2209–2244.
- (161) de Voors, A. C. A.; Koper, M. T. M.; van Santen, R. A.; van Veen, J. A. R. Mechanistic study on the electrocatalytic reduction of nitric oxide on transition-metal electrodes. *J. Catal.* **2001**, *202* (2), 387–394.
- (162) de Voors, A. C. A.; Koper, M. T. M.; van Santen, R. A.; van Veen, J. A. R. Mechanistic study of the nitric oxide reduction on a polycrystalline platinum electrode. *Electrochim. Acta* **2001**, *46* (6), 923–930.
- (163) Sa, J.; Montero, J.; Duncan, E.; Anderson, J. A. Bi modified Pd/SnO<sub>2</sub> catalysts for water denitration. *Appl. Catal., B* **2007**, *73* (1–2), 98–105.
- (164) Pintar, A.; Setinc, M.; Levec, J. Hardness and salt effects on catalytic hydrogenation of aqueous nitrate solutions. *J. Catal.* **1998**, *174* (1), 72–87.
- (165) Ranea, V. A.; Strathmann, T. J.; Shapley, J. R.; Schneider, W. F. DFT comparison of *N*-nitrosodimethylamine decomposition pathways over Ni and Pd. *ChemCatChem* **2011**, *3* (5), 898–903.
- (166) Figueras, F.; Coq, B. Hydrogenation and hydrogenolysis of nitro-, nitroso-, azo-, azoxy- and other nitrogen-containing compounds on palladium. *J. Mol. Catal. A: Chem.* **2001**, *173* (1–2), 223–230.
- (167) Patel, R.; Suresh, S. Decolourization of azo dyes using magnesium-palladium system. *J. Hazard. Mater.* **2006**, *137* (3), 1729–1741.
- (168) Levenspiel, O. *Chemical Reaction Engineering*; John Wiley & Sons: New York, 1972; Chapter 14: Solid-Catalyzed Reactions, 2nd ed.
- (169) Hayduk, W.; Laudie, H. Prediction of diffusion-coefficients for nonelectrolytes in dilute aqueous-solutions. *AIChE J.* **1974**, *20* (3), 611–615.
- (170) Davie, M. G.; Cheng, H. F.; Hopkins, G. D.; Lebron, C. A.; Reinhard, M. Implementing heterogeneous catalytic dechlorination technology for remediating TCE-contaminated groundwater. *Environ. Sci. Technol.* **2008**, *42* (23), 8908–8915.
- (171) Knitt, L. E.; Shapley, J. R.; Strathmann, T. J. Rapid metal-catalyzed hydrodehalogenation of iodinated X-ray contrast media. *Environ. Sci. Technol.* **2008**, *42* (2), 577–583.
- (172) Pintar, A.; Batista, J.; Musevic, I. Palladium-copper and palladium-tin catalysts in the liquid phase nitrate hydrogenation in a batch-recycle reactor. *Appl. Catal., B* **2004**, *52* (1), 49–60.
- (173) Witonska, I.; Karski, S.; Goluchowska, J. Hydrogenation of nitrate in water over bimetallic Pd-Ag/Al<sub>2</sub>O<sub>3</sub> catalysts. *React. Kinet. Catal. Lett.* **2007**, *90* (1), 107–115.
- (174) Yuan, G.; Keane, M. A. Aqueous-phase hydrodechlorination of 2,4-dichlorophenol over Pd/Al<sub>2</sub>O<sub>3</sub>: Reaction under controlled pH. *Ind. Eng. Chem. Res.* **2007**, *46* (3), 705–715.
- (175) Lowry, G. V.; Reinhard, M. Pd-catalyzed TCE dechlorination in groundwater: Solute effects, biological control, and oxidative catalyst regeneration. *Environ. Sci. Technol.* **2000**, *34* (15), 3217–3223.
- (176) Munakata, N.; Reinhard, M. Palladium-catalyzed aqueous hydrodehalogenation in column reactors: Modeling of deactivation kinetics with sulfide and comparison of regenerants. *Appl. Catal., B* **2007**, *75*, 1–10.
- (177) Hildebrand, H.; Mackenzie, K.; Kopinke, F. D. Pd/Fe<sub>3</sub>O<sub>4</sub> nano-catalysts for selective dehalogenation in wastewater treatment processes-Influence of water constituents. *Appl. Catal., B* **2009**, *91* (1–2), 389–396.
- (178) Kopinke, F. D.; Angeles-Wedler, D.; Fritsch, D.; Mackenzie, K. Pd-catalyzed hydrodechlorination of chlorinated aromatics in contaminated waters-Effects of surfactants, organic matter and catalyst protection by silicone coating. *Appl. Catal., B* **2010**, *96* (3–4), 323–328.
- (179) Lecloux, A. J. Chemical, biological and physical constraints in catalytic reduction processes for purification of drinking water. *Catal. Today* **1999**, *53* (1), 23–34.
- (180) Licht, S. Aqueous solubilities, solubility products and standard oxidation-reduction potentials of the metal sulfides. *J. Electrochem. Soc.* **1988**, *135* (12), 2971–2975.
- (181) Chaplin, B. P.; Shapley, J. R.; Werth, C. J. The selectivity and sustainability of a Pd-In/gamma-Al<sub>2</sub>O<sub>3</sub> catalyst in a packed-bed reactor: The effect of solution composition. *Catal. Lett.* **2009**, *130* (1–2), 56–62.
- (182) Pintar, A.; Vetinc, M.; Levec, J. Hardness and salt effects on catalytic hydrogenation of aqueous nitrate solutions. *J. Catal.* **1998**, *174* (1), 72–87.
- (183) Peljhan, S.; Kokalj, A. Adsorption of chlorine on Cu(111): A density-functional theory study. *J. Phys. Chem. C* **2009**, *113* (32), 14363–14376.
- (184) Ordóñez, S.; Vivas, B. P.; Diez, F. V. Minimization of the deactivation of palladium catalysts in the hydrodechlorination of trichloroethylene in wastewaters. *Appl. Catal., B* **2010**, *95* (3–4), 288–296.
- (185) de Pedro, Z. M.; Diaz, E.; Mohedano, A. F.; Casas, J. A.; Rodriguez, J. J. Compared activity and stability of Pd/Al<sub>2</sub>O<sub>3</sub> and Pd/AC catalysts in 4-chlorophenol hydrodechlorination in different pH media. *Appl. Catal., B* **2011**, *103* (1–2), 128–135.
- (186) Shindler, Y.; Matatov-Meytal, Y.; Sheintuch, M. Wet hydrodechlorination of p-chlorophenol using Pd supported on an activated carbon cloth. *Ind. Eng. Chem. Res.* **2001**, *40*, 3301.
- (187) Gammons, C. H. Experimental investigations of the hydrothermal geochemistry of platinum and palladium. 5. Equilibria between platinum metal, Pt(II), and Pt(IV) chloride complexes at 25 to 300 degrees C. *Geochim. Cosmochim. Acta* **1996**, *60* (10), 1683–1694.
- (188) van Middlesworth, J. M.; Wood, S. A. The stability of palladium(II) hydroxide and hydroxy-chloride complexes: An experimental solubility study at 25–85 degrees C and 1 bar. *Geochim. Cosmochim. Acta* **1999**, *63* (11–12), 1751–1765.

- (189) Beamish, F. E.; Dale, J. Determination of palladium by means of potassium iodide. *Indust. Eng. Chem. Anal. Ed.* **1938**, *10* (12).
- (190) Munakata, N.; Cunningham, J. A.; Reinhard, M.; Ruiz, R.; Lebron, C. Palladium catalysis horizontal-flow treatment wells: Field-scale design and laboratory study. In *Proceedings of the Third International Conference on Remediation of Chlorinated and Recalcitrant Compounds*, Monterey, CA; Gavaskar, A., Chen, A., Eds.; Battelle Press: Columbus, OH, 2002.
- (191) McNab, J. W. W.; Ruiz, R.; Reinhard, M. In-situ destruction of chlorinated hydrocarbons in groundwater using catalytic reductive dehalogenation in a reactive well: Testing and operational experiences. *Environ. Sci. Technol.* **2000**, *34* (1), 149–153.
- (192) Schuth, C.; Kummer, N. A.; Weidenthaler, C.; Schad, H. Field application of a tailored catalyst for hydrodechlorinating chlorinated hydrocarbon contaminants in groundwater. *Appl. Catal., B* **2004**, *52* (3), 197–203.
- (193) Palomares, A. E.; Franch, C.; Corma, A. Nitrates removal from polluted aquifers using (Sn or Cu)/Pd catalysts in a continuous reactor. *Catal. Today* **2010**, *149* (3–4), 348–351.
- (194) Fritsch, D.; Kuhr, K.; Mackenzie, K.; Kopinke, F. D. Hydrodechlorination of chloroorganic compounds in ground water by palladium catalysts - Part I. Development of polymer-based catalysts and membrane reactor tests. *Catal. Today* **2003**, *82* (1–4), 105–118.
- (195) Heck, K. N.; Nutt, M. O.; Alvarez, P.; Wong, M. S. Deactivation resistance of Pd/Au nanoparticle catalysts for water-phase hydrodechlorination. *J. Catal.* **2009**, *267* (2), 97–104.
- (196) Fang, Y. L.; Miller, J. T.; Guo, N.; Heck, K. N.; Alvarez, P. J. J.; Wong, M. S. Structural analysis of palladium-decorated gold nanoparticles as colloidal bimetallic catalysts. *Catal. Today* **2011**, *160* (1), 96–102.
- (197) Chaplin, B. P.; Shapley, J. R.; Werth, C. J. Oxidative regeneration of sulfide-fouled catalysts for water treatment. *Catal. Lett.* **2009**, *132* (1–2), 174–181.
- (198) Angeles-Wedler, D.; Mackenzie, K.; Kopinke, F.-D. Sulphide-induced deactivation of Pd/Al<sub>2</sub>O<sub>3</sub> as hydrodechlorination catalyst and its oxidative regeneration with permanganate. *Appl., Catal. B* **2009**, *90*, 613–617.
- (199) Angeles-Wedler, D.; MacKenzie, K.; Kopinke, F. D. Permanganate oxidation of sulfur compounds to prevent poisoning of Pd catalysts in water treatment processes. *Environ. Sci. Technol.* **2008**, *42* (15), 5734–5739.
- (200) McNab, W. W.; Ruiz, R.; Reinhard, M. In-situ destruction of chlorinated hydrocarbons in groundwater using catalytic reductive dehalogenation in a reactive well: Testing and operational experiences. *Environ. Sci. Technol.* **2000**, *34* (1), 149–153.
- (201) Love, J. C.; Wolfe, D. B.; Haasch, R.; Chabiny, M. L.; Paul, K. E.; Whitesides, G. M.; Nuzzo, R. G. Formation and structure of self-assembled monolayers of alkanethiolates on palladium. *J. Am. Chem. Soc.* **2003**, *125* (9), 2597–2609.
- (202) Choudhary, V. R.; Samanta, C. Role of chloride or bromide anions and protons for promoting the selective oxidation of H<sub>2</sub> by O<sub>2</sub> to H<sub>2</sub>O<sub>2</sub> over supported Pd catalysts in an aqueous medium. *J. Catal.* **2006**, *238* (1), 28–38.
- (203) Pauer, G.; Winkler, A. Water formation on Pd(111) by reaction of oxygen with atomic and molecular hydrogen. *J. Chem. Phys.* **2004**, *120* (8), 3864–3870.
- (204) Bayer, P.; Schuth, C. Technico-economic assessment of groundwater treatment by palladium-on-zeolite-catalyst in comparison to gac fixed bed adsorbers. *Water Sci. Technol.* **2010**, *62* (3), 708–718.
- (205) Pintar, A.; Batista, J.; Levec, J. Catalytic denitrification: Direct and indirect removal of nitrates from potable water. *Catal. Today* **2001**, *66* (2–4), 503–510.
- (206) Pintar, A.; Batista, J.; Levec, J. Integrated ion exchange/catalytic process for efficient removal of nitrates from drinking water. *Chem. Eng. Sci.* **2001**, *56* (4), 1551–1559.
- (207) Pintar, A.; Batista, J. Improvement of an integrated ion-exchange/catalytic process for nitrate removal by introducing a two-stage denitrification step. *Appl. Catal., B* **2006**, *63* (1–2), 150–159.
- (208) Luo, Y. R. *Comprehensive Handbook of Chemical Bond Energies*; CRC Press: Boca Raton, FL, 2007.
- (209) Desai, E.; Wentworth, W. E.; Chen, E. C. M. Thermal electron attachment to chloro- and bromoethylenes: The demonstration of a new electron capture detector mechanism. *J. Phys. Chem.* **1988**, *92* (2), 286.
- (210) Liu, Z. J.; Betterton, E. A.; Arnold, R. G. Electrolytic reduction of low molecular weight chlorinated aliphatic compounds: Structural and thermodynamic effects on process kinetics. *Environ. Sci. Technol.* **2000**, *34* (5), 804–811.